

https://dspace.org/

Determining the switching impulse breakdown voltage over large air gaps with an application to tower-conductor window configurations

Ehlers, Richard

1998

http://hdl.handle.net/10539/22712

Ehlers, Richard (1998) Determining the switching impulse breakdown voltage over large air gaps with an application to tower-conductor window configurations, University of the Witwatersrand, Johannesburg, <http://hdl.handle.net/10539/22712>

Downloaded from a DSpace repository. https://dspace.org/

Determining the switching impulse breakdown voltage over large air gaps with an application to tower-conductor window configurations

Richard Ehlers

A dissertation submitted to the Faculty of Engineering, University of the Witwatersrand, in fulfilment of the requirements for the degree of Master of Science in Engineering

February 20th, 1998

DECLARATION

I declare that this research report is my own, unaided work. It is being submitted for the degree of Master of Science in Engineering at the University of the Witwatersrand, Johannesburg. To my knowledge, it has not been submitted before for any degree or examination at any other university.

SIGNED : _____

DATE : 20-2-98

Abstract

An available model used to determine the 50% breakdown voltage for rod-type and conductor-type gaps subject to switching impulse waveforms has been applied to a tower-conductor window gap configuration. The results for rod-plane, conductor-plane and tower-conductor window gaps have all been compared and correspond well with practical data. In order to apply the model, a charge simulation technique has been adopted in conjunction with the 'Coulomb 3D' charge simulation package. Additional tests have been performed where parameters of the charge simulation method and the electrode geometry have been adjusted and consequent conclusions made. Recommendations for further application of the model have been suggested.

Contents

LIST OF FIGURES v

LIST OF TABLES v

1. INTRODUCTION 1

2. OUTLINE OF RESEARCH 3

2.1 Problem Statement 3
2.2 Background 3
2.3 The Research Process 7

3. THE ROD-PLANE GAP 9

3.1 The Continuous Leader Inception Voltage 9
3.1.1 Model for the Rod-Plane Gap 9
3.1.2 Prediction of Leader Inception Voltage 10
3.1.2.1 A 3m Rod-Plane Gap 10
3.1.2.2 A 7m Rod-Plane Gap 12
3.2 The Leader Voltage Drop 13
3.3 The Breakdown Voltage 14

4. THE CONDUCTOR-PLANE GAP 17

4.1 The Continuous Leader Inception Voltage 17
4.1.1 Model for the Conductor-Plane Gap 17
4.1.2 Prediction of Leader Inception Voltage 20
4.1.2.1 A 2m Conductor-Plane Gap 20
4.1.2.2 A 6m Conductor-Plane Gap 22
4.2 The Leader Voltage Drop 23
4.3 The Breakdown Voltage 23

5. THE TOWER-CONDUCTOR GAP 26

5.1 The Continuous Leader Inception Voltage 26
5.1.1 Model for the Tower-Conductor Gap 26
5.1.2 Prediction of Leader Inception Voltage 28
5.1.2.1 A 5m Tower-Conductor Gap 28
5.1.2.2 A 9.3m Tower-Conductor Gap 30
5.2 The Leader Voltage Drop 31
5.3 The Breakdown Voltage 31

6. SUMMARY AND RECOMMENDATIONS 34

6.1 SUMMARY 34
6.2 RECOMMENDATIONS 36
ACKNOWLEDGEMENTS 38
REFERENCES 39
APPENDIX A 42
APPENDIX B 76
APPENDIX C 87
APPENDIX D 116

List of Figures

FIGURE 2.1 - COMPARISON OF THE POSITIVE AND NEGATIVE STREAMER CHANNEL 4
FIGURE 3.1 - MODEL OF THE ROD-PLANE GAP 10
FIGURE 3.2 - TOTAL INDUCED VOLTAGE FOR THE 3M ROD-PLANE GAP 11
FIGURE 3.3 - TOTAL INDUCED VOLTAGE FOR THE 7M ROD-PLANE GAP 13
FIGURE 4.1 - TOTAL INDUCED VOLTAGE FOR THE 2M CONDUCTOR-PLANE GAP 21
FIGURE 4.2 - TOTAL INDUCED VOLTAGE FOR THE 6M CONDUCTOR-PLANE GAP 22
FIGURE 5.1 - MODEL FOR THE TOWER-CONDUCTOR WINDOW GAP 27
FIGURE 5.2 - TOTAL INDUCED VOLTAGE FOR THE 5M TOWER-CONDUCTOR GAP 29
FIGURE 5.3 - TOTAL INDUCED VOLTAGE FOR THE 9.3M TOWER-CONDUCTOR GAP 30
FIGURE B.1 - CONTINUOUS LEADER INCEPTION 76
FIGURE B.2 - THE CHARGE SIMULATION TECHNIQUE 82

List of Tables

TABLE 3.1 - ROD-PLANE COMPARISON BETWEEN THEORY AND MEASURED U_{50} VALUES 15
TABLE 3.2 - COMPARISON BETWEEN THEORY AND THE CHARGE SIMULATION TECHNIQUE 15
TABLE 4.1 - CONDUCTOR-PLANE COMPARISON BETWEEN THEORY AND MEASURED U_{50} VALUES 24
TABLE 5.1 - TOWER-CONDUCTOR COMPARISON BETWEEN THEORY AND MEASURED U_{50} VALUES 32

1. Introduction

Flashovers are likely to occur on transmission lines as a result of lightning strikes, switching operations or power frequency overvoltages. Any of these sources may result in either a phase-phase or phase-ground breakdown occurring on the line. Such a breakdown which consequently leads to a loss of power on the line is very costly to the supplier of electricity and more importantly to the customer, especially where the industrial operations of the customer are reliant on the uninterrupted supply of electricity. Furthermore, breakdowns can lead to damage of equipment and property and in some circumstances lead to the loss of life. Hence, it is important that all necessary and possible precautions are taken to prevent flashovers from occurring.

This dissertation investigates breakdowns over long air-gaps specifically due to switching operations where the magnitude of the transient impulse on line caused by the switching operation is sufficient to ionise the air around the line to such an extent that the streamer produced is able to develop into a leader which rapidly propagates to a neighbouring phase conductor or ground. Of particular interest in this study is the tower-conductor window geometry where the flashover occurs from the conductor to the tower window.

Extensive work has already been done into the physical processes that govern discharges in large air-gaps with the intention of predicting, to a satisfactory level of accuracy, whether the dielectric strength of the insulating air is sufficient to prevent a breakdown from occurring under impulsive conditions. A background to this work is provided in the next chapter. Most of the work available has been harnessed and analysed in search for a mathematical model that will accurately predict the insulating strength for a tower-conductor window geometry. The emphasis of this investigation is then to apply and verify a mathematical model by comparing it to practical results which are extensively available. *Chapter 2* discusses further how this is done.

In *Chapter 3*, the first of three geometric models, the rod-plane gap is studied in order to verify the mathematical model for the simplest geometry where simulation results are

compared with easily derived analytical calculations. The calculated breakdown voltage is then also verified using practical data. Once the validity of the model is confirmed for a simple geometry, more complex geometries can then be studied.

Chapter 4 deals with the conductor-plane gap where the model is again verified by comparing the simulation results with measured voltage flashover values. The analytical calculations for the conductor-plane gap are far more complex than those for the rod-plane gap and hence the researcher relies solely on simulation to verify the mathematical model. Thus, it is essential that there is confidence in the simulation process, which is the main purpose for studying the rod-plane gap where analytical methods are available for verification.

Since the model being investigated is suited for rod-plane and conductor-plane type geometry's, once the model has been verified for the rod-plane and conductor-plane gaps, the next step of verifying the model for a tower-conductor window gap is pursued. This is done in *Chapter 5*. The tower-conductor gap is a modification of the conductor-plane gap, thus allowing for the validated model of the conductor-plane gap to be used to obtain and predict breakdown values for the tower-conductor window configuration.

The report concludes by summarising the findings of the research undertaken. Areas for further study are suggested.

2. Outline of Research

2.1 Problem Statement

The aim of the research work is to predict the breakdown voltage, to a sufficient level of accuracy, for a tower-conductor window configuration where the conductor is subject to switching impulses. It is intended that a model be produced or an existing model verified so that the anticipated flashover value can be predicted for a defined gap distance and for the given electrode dimensions of the tower and the conductor.

2.2 Background

A great deal of work has already been done in investigating the physical processes of leader breakdown due to switching impulses as well as in performing measurements of breakdown values for a wide range of electrode geometry's and gap distances. This has led to a limited number of theoretical models and a large number of empirical formulas which attempt to define the breakdown voltage. A summary of the work available to date in this subject is provided in *Appendix A*.

The breakdown voltage under switching impulse conditions varies with polarity. In general the positive breakdown voltage is lower than the negative breakdown voltage except in certain circumstances such as where live line working is performed on complex geometry's [Sadurski, van der Merwe, Muftic], at low air pressures (below 5bar) [Kuffel & Zaengl], in conductor-rod gaps where the length of the rod exceeds the gap length and under wet conditions [Paris]. The physical reason for the positive breakdown voltage generally being lower than the negative breakdown voltage is explained as follows : for a positive point-plane gap, electrons formed in an avalanche are as a result of the high mobility ions drawn into the anode, leaving the positive space charge behind. This causes a reduction in the field strength close to the anode and an increase further away from it

which favours breakdown. For a negative point-plane gap, the opposite occurs where electrons are repelled from the point into the low field region giving rise to an enhanced field at the point but resulting in a reduced ionisation region. The positive space charge formed has a cancellation effect which consequently terminates the ionisation. To overcome this retarding cancellation process a higher voltage is required and hence negative breakdown occurs at a higher voltage than positive breakdown. Furthermore, positive streamers directed towards the cathode have a narrower channel compared to the negative, anode directed streamers and therefore result in a higher local gradient [Niemeyer, Ullrich, Wiegart]. Hence the positive streamer is more likely to propagate in weaker background fields than the negative streamer. The situation is shown in *Figure 2.1* where the positive streamer channel diameter is approximately one third of that of the negative streamer channel. The narrower channel for positive streamers is due to the centering effect of individual avalanches which converge at the streamer head. In the case of negative streamers, a wider channel is formed when photons and avalanches emerging from the streamer head cause the ionisation to spread more radially.
As a result, in determining the critical breakdown voltage, researchers have mainly focused on breakdowns under positive switching impulse conditions.

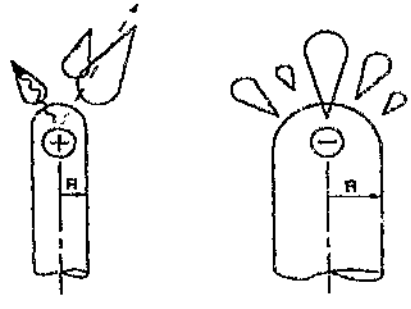

Figure 2.1 – Comparison of the Positive and Negative Streamer Channel

The breakdown voltage is also influenced by the waveshape of the impulse. As the leader propagates through the gap prior to breakdown the E-field collapses thus resulting in a lower breakdown voltage with an increasing front of the impulse. As a result of the leader ageing, the breakdown voltage starts to increase after a certain lifetime of the leader. Hence, a minimum value of the breakdown voltage exists for a certain gap length which

corresponds to a critical time where the leader is active [Gallimberti]. This time is known as the critical time to crest of the switching impulse. For a faster rising impulse, the space charge formation on the front will be negligible with the result that there is little field modification due to space charge. However, despite this, the leader processes will not have enough time to develop and thus a higher applied voltage would be required if breakdown were to occur. On the contrary, with a slower rising impulse, there will be significant space charge injection associated with leader inception to inhibit further streamer development. This is due to a sufficient time difference between the leader inception and the onset of continuous leader inception, the two being approximately coincidental in the case of faster rising impulses [Rizk]. A higher applied voltage would once again be required to support continuous leader propagation. Hence, a critical time exists for a certain applied voltage to overcome the effects of space charge, yet still allow sufficient time for the leader processes to develop such that breakdown of the air gap occurs.

The effects of atmospheric conditions also need to be considered when determining the breakdown voltage. Usually, the flashover voltage for a given path in air is raised by an increase either in air density or the humidity [Aihara et al.].

From the models available, the work of Rizk [Rizk Jan. 1989, Rizk Oct. 1989] best suited the requirements for attempting to predict the breakdown voltage of a tower-conductor window geometry. This can be understood based on the developments of various models as outlined in *Appendix A*. Rizk's work originated from a crude model by Paris which was improved upon by authors Gallet, Leroy, Lacey and Kromer. Their work formed the foundation for the model from Carrara and Thione which was later refined by Rizk. Furthermore, the work of Rizk, based on its evolution on previous models, has been shown to fit a variety of geometric configurations satisfactorily. A brief introduction to the work of Rizk is now presented but the reader is advised to refer to *Appendix B* for a detailed analysis of Rizk's work.

Rizk developed a model which can be used to predict the breakdown voltage of a long air-gap subject to a positive switching impulse, based on the critical time to crest. The model is presented for rod-plane and conductor-plane geometry's but can be applied to

rod-type and conductor-type configurations. The breakdown voltage is made up of two components, the continuous leader inception voltage and the leader voltage drop. The sum of these two components provide the minimum voltage at which flashover will occur. However, as the flashover voltage is variable, the predicted breakdown voltage required is the 50% flashover voltage value which is defined as the value where 50 of 100 applications of the same voltage will lead to a breakdown.

The continuous leader inception voltage is defined in *equation 2.1* and is the general form of the equation which can be applied to a variety of rod-type and conductor-type geometry's by subsituting for the unknown parameter *R*.

$$U_k = \frac{U_{cr}}{1 + \frac{A}{R}} \tag{2.1}$$

The parameter U_{cr} is a constant which has the value of 1556kV and 2247kV for rod-type and conductor-type configurations respectively. The parameter A is a constant which has the value of 7.78m for a rod-type geometry. For a conductor-type geometry, the value of A depends on how the geometric model is defined and is described in more detail in *Chapter 4*. The parameter R is a function of the gap geometry, the gap spacing, the nature and dimensions of the ground electrode and any surrounding objects. It has the dimensions of metres and can either be determined analytically or, in the case of complex geometry's, more conveniently by charge simulation. By including the parameter R, Rizk has accounted for the influence of image charges as a result of the space charges that are produced by streamers prior to the formation of a leader.

The leader voltage drop is defined in *equation 2.2* and has the dimensions of kilovolt. The voltage drop is a function of the rod-plane gap distance, d, and the leader length, l_s, which is the maximum leader length prior to the final jump of the leader that consequently bridges the gap to result in total breakdown of the gap.

$$\Delta U_l = 50 l_s + 37.5 \ln[8 - 7\exp(\frac{-1.33d}{1 + \frac{3.89}{d}})] \tag{2.2}$$

With the minimum breakdown voltage, U_0, being the sum of the continuous leader inception voltage and the leader voltage drop, the 50% breakdown voltage is derived as shown in *equation 2.3*.

$$U_{50} = \frac{U_0}{1 - 3\sigma} \tag{2.3}$$

The standard deviation in the breakdown voltage is given by the parameter σ which assumes a value, generally in the range 0.03-0.05, depending on the type of geometry. [Rizk, Jan 1989][Carrara & Thione],[Rizk, Oct 1989]

2.3 The Research Process

In solving the problem at hand of obtaining a model which will satisfactorily allow the breakdown voltage of a tower-conductor window to be determined when subjected to a positive switching impulse, three areas need to be addressed in the research process.

The first is to acquire and analyse the work available in the field of study. This will provide a broad background which can at a later stage in the research process be used to compare and validate any results or conclusions. The literature survey which is listed in *Appendix A* contains descriptions of the physical processes involved in discharges, empirical formulas and models for switching impulse flashovers. The most relevant work, namely that of Rizk provides a basis from which to launch into the second stage of the research.

With a model available which has briefly been described in section *2.2 Background*, the second stage of the research process, which is to accurately test and verify the model being used, starts to rely heavily on simulation tools. In order to obtain a value for R when determining the continuous leader inception voltage, two finite element packages were used. The first package, *Maxwell 2D* and its 3D version, *Maxwell 3D* [Ansoft] were initially used in trying to verify R for the rod-plane case where results obtained from

simulation could be compared to the analytically expected results. When unsatisfactory results for the rod-plane case were obtained from the *Maxwell* packages, a 3D Boundary Element Method software package, *Coulomb* [I.E.S.] was used for the electric field simulations that gave satisfactory results. With the rod-plane case verified based on analytical expectations the confidence was provided to study the conductor-plane and tower-conductor window geometry's by using *Coulomb*.

The final stage of the research process relies on recorded experimental data where switching impulse flashovers have occurred. The model of Rizk is used to obtain breakdown values for the conductor-plane geometry which are then compared with the experimental data. Only once the model, which has been specifically derived for rod-plane and conductor-plane geometry's, has been satisfactorily tested and verified for those geometry's, is the test that the model can be applied to rod-type and conductor-type geometry's confidently tested by using the tower-conductor window geometry. The simulation results using *Coulomb* are compared with recorded flashover values and conclusions on the applicability of the model are made.

3. The Rod-Plane Gap

The rod-plane gap is one of the simplest geometric configurations used in high voltage and as a result is often used as a reference geometry for more complex geometry's. A good example is with the concept of a gap factor which is 1 for the rod-plane geometry and greater than 1 for other geometry's where the breakdown voltage is higher than that of the rod-plane gap. The rod-plane gap has a lower breakdown voltage relative to other more complex geometry's due to the high gradient of the E-field around the rod tip. The rod tip may also have a variety of shapes such as spherical or conical which also affect the gradient of the E-field and thus the breakdown voltage.

3.1 The Continuous Leader Inception Voltage

3.1.1 Model for the Rod-Plane Gap

In solving for the continuous leader inception voltage as given by *equation B.10*, only one unknown, R, needs to be determined. The parameters of $U_{c\infty}$ and A have previously been calculated by Rizk [Rizk Jan. 1989] who has in turn used experimental data from work done on the switching surge strength of large air gaps [Carrara & Thione]. Based on Rizk's work, the parameters for $U_{c\infty}$ and A assume the values of 1556kV and 7.72m respectively.

The unknown, R, is obtained using a charge simulation technique which is described in *Appendix B.2*. The rod and space charge together with their respective image charges are shown in *Figure 3.1*. Parameters are defined in *Appendix B.2*. It is important to remember that by specifying an image rod and an image charge, the ground plane is automatically defined and hence there is no need to include it.

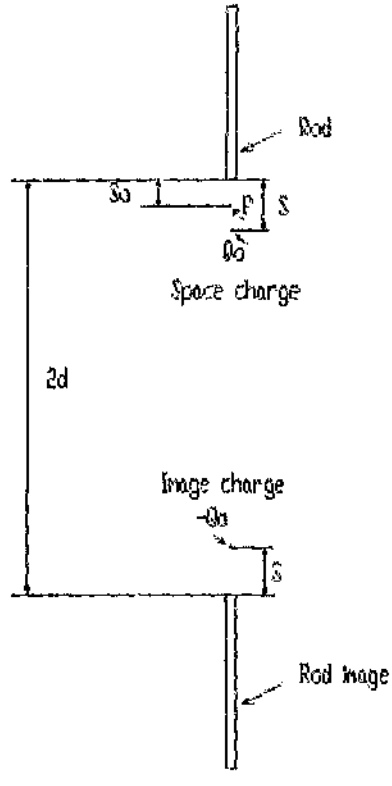

Figure 3.1 - Model of the Rod-Plane Gap

3.1.2 Prediction of Leader Inception Voltage

3.1.2.1 A 3m Rod-Plane Gap

The first test on the rod-plane gap was done with a 3m gap between the rod tip and the plane. The rod had a 5mm radius and was modelled as a copper cylinder with a flat tip having a relative permittivity of 1 and a conductivity of 5.8e7S. A distance, *s*, of 100mm was used between the rod tip and the centre of the space charge, the latter being modelled as a perfectly conducting sphere with a 1mm radius, having a charge, Q_s, of 5μC and a relative permittivity of 1. When specifying the number of elements to be used for the rod, space charge and their images, 8192 elements were used. This is the maximum number of elements that *Coulomb* is capable of using. The total induced voltage due to space charge

is measured at a point P where s_m is 20mm from the tip of the rod. It is necessary to note at this point that the choice of magnitude for the space charge is arbitrary as is verified in *Appendix D.1.2*. This is because the image charge is scaled by the same magnitude as the space charge. The values for s and s_m are also arbitrary with the only restriction that Rizk imposes being that they must be significantly smaller than the gap distance. This is verified in *Appendix D.1.1* where it is shown that as the value of s increases such that it is no longer much smaller than the gap distance, the accuracy of the charge simulation method is reduced. The value of s_m is of the order of s and was chosen to be at a point where the space charge E-field had attenuated significantly rather than where the E-field was high as the latter would have given rise to sensitive induced voltage values.

All results from the simulation can be found in *Appendix C*. For this first test on the rod-plane gap, the results taken from *Appendix C.1.1* for the magnitude of the total streamer space charge induced voltage with respect to height above the ground plane between the space charge and the rod tip have been plotted in *Figure 3.2*.

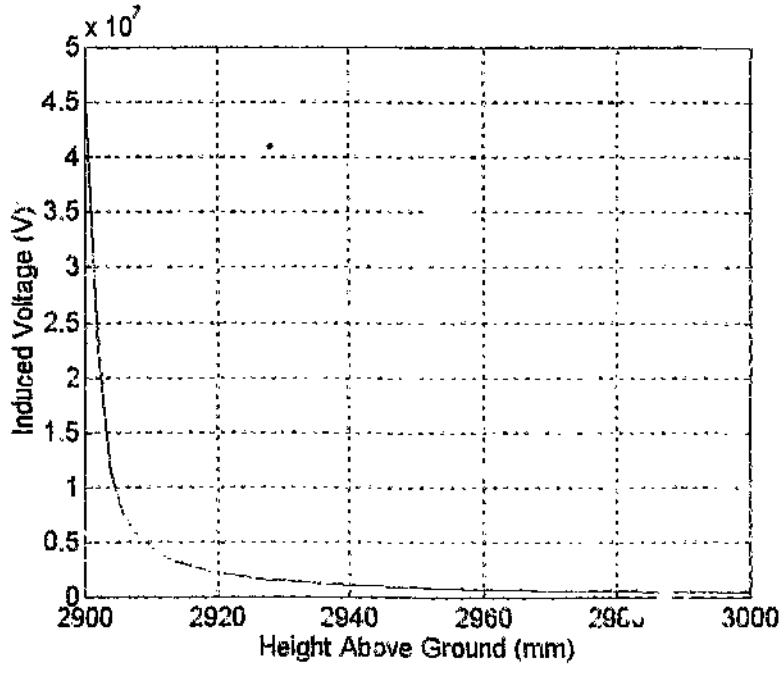

Figure 3.2 - Total Induced Voltage for the 3m Rod-Plane Gap

From *Figure 3.2* and more precisely from the data printout in *Appendix C.1.1*, the magnitude of the total induced voltage, U_m, at the point P, 80mm from the centre of the space charge or 2980mm above the ground, is 554.1kV. With reference to *equation B.8*, the total induced voltage is represented as follows :

$$U_m = \frac{Q}{4\pi} \left(\frac{}{s_n} \right) - \frac{Q_o}{4\pi\varepsilon_0 R}$$

It should be noted that the measured potential due to space charge that is induced on the high voltage rod as a result of the direct influencing charge, Q_o, is rather small because of the small surface area of the rod. Thus, most of the potential making up the term, U_m, is as a result of the image charges of Q_o.

Substituting values for U_m, Q_o, s and s_n, the magnitude of R is calculated as 5.685m. With the known values of $U_{c.c}$ and A for the rod-plane gap as 1556kV and 7.78m respectively, the continuous leader inception voltage, U_0, is calculated using *equation B.10* to be 657.0kV.

3.1.2.2 A 7m Rod-Plane Gap

The second test on the rod-plane gap was the same as the first test except for the fact that the gap length was increased from 3m to 7m.

The total induced voltage measured between the rod and the space charge with respect to the height of the rod above the ground can be found in *Appendix C.1.2* and is plotted in *Figure 3.3*.

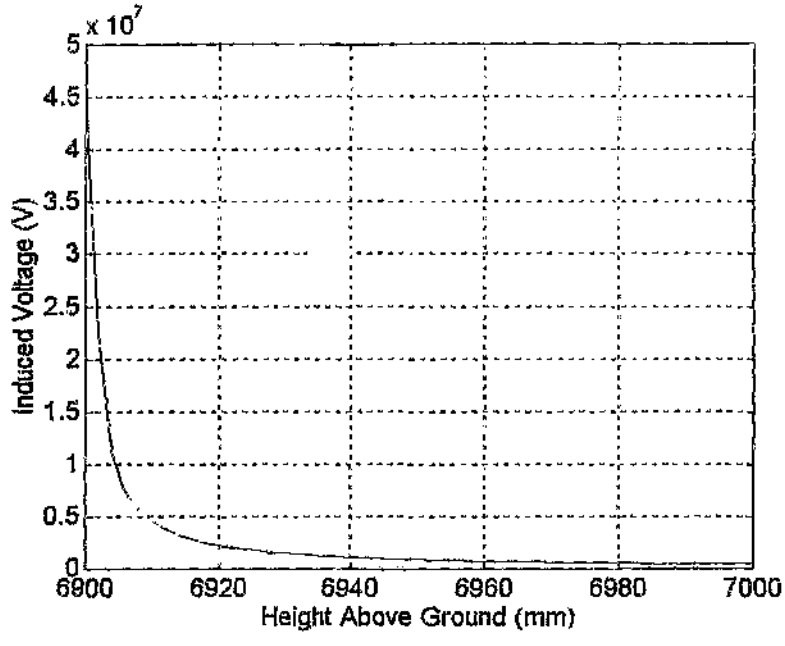

Figure 3.3 - Total Induced Voltage for the 7m Rod-Plane Gap

The total induced voltage, U_m, at the point P, a distance 20mm from the high voltage electrode or 80mm from the centre of the space charge, is 558.5kV. Substituting for U_m, Q_p, s and s_p into *equation B.8*, the value of R is evaluated as 12.83m. The magnitude of the continuous leader inception voltage is then calculated from *equation B.10* to be 968.6kV.

3.2 The Leader Voltage Drop

The voltage drop in the leader can be determined for any leader length, l_s, by using *equation B.19*.

The leader length for a 3m rod-plane gap is calculated from *equation B.18* to be 1.30cm and substituting for l_s into *equation B.19*, the leader voltage drop, ΔU_s is 137.0kV.

For the 7m rod-plane gap the leader length is 4 500m and hence the leader voltage drop is 302.9kV.

3.3 The Breakdown Voltage

With the continuous leader inception voltage, U_k, and the leader voltage drop, ΔU_l, known for both the 3m and 7m rod plane gaps, the minimum breakdown voltage, U_B, is determined as their sum :

$$\Rightarrow \text{3m Rod-Plane Gap : } U_B = U_k + \Delta U_l = 657.0\text{kV} + 137.0\text{kV}$$
$$= 794.0\text{kV}$$

$$\Rightarrow \text{7m Rod-Plane Gap : } U_B = U_k + \Delta U_l = 968.6\text{kV} + 302.9\text{kV}$$
$$= 1272\text{kV}$$

The 50% breakdown voltage, U_{50}, is calculated from the minimum breakdown voltage using *equation B.22* with a statistical variation, $\sigma = 5\%$ for rod-type gaps [Rizk, Jan 1989][Carrara and Thione]. Thus, the U_{50} values for the 3m and 7m gaps are 934.1kV and 1496kV respectively. These values for the U_{50} are compared in *Table 3.1* with measured values of the U_{50} for the 3m gap [Harada, Aihara & Aoshima] and the 7m gap [Berger, et al.] where breakdowns have occurred in practice. Both the data for the 3m and the 7m gaps have been obtained with critical time to crest waveforms. Corrections for humidity and relative air density have been made for the 3m gap data whilst for the 7m gap, the lowest set of data have been taken as no data with humidity and relative air density corrections existed in the available literature. However, were these corrections to be made such that the measured breakdown voltage drops, it would aid to reduce to the percentage difference between Rizk's model and the measured data with the result that no confidence would be lost with the Rizk model. If the corrections were to increase the measured voltage data, the Rizk model would remain a safe and suitable means of establishing a minimum clearance distance.

	Predicted, using R	Measured	Percentage difference
3m Rod-Plane Gap	934.1kV	943kV	0.95%
7m Rod-Plane Gap	1496kV	1555kV	3.8%

Table 3.1 - Rod-Plane Comparison Between Theory and Measured U_{50} Values

From *Table 3.1* it can be seen that the U_{50} voltages correspond fairly well between the predicted and measured values. Furthermore, the predicted values are conservative and thus would make the model of the rod-plane gap a useful tool for design purposes.

Table 3.2 provides a comparison between *equation B.10* where firstly the theoretical value for R equal to $2d$ is used and then when the refined value of R from the charge simulation technique is used. It can be seen that there is very little error in using the theoretical value for R equal to $2d$, but using a refined value for R results in a conservative value for the U_{50} voltage and thus is an improvement in terms of calculating safe clearance distances.

	Calculated, using R equal to 2d	Predicted, using refined value of R	Percentage difference
3m Rod-Plane Gap	958.2kV	934.1kV	2.52%
7m Rod-Plane Gap	1533kV	1496kV	2.41%

Table 3.2 - Comparison Between Theory and the Charge Simulation Technique

In addition to the two tests performed with varying gap distances in the rod-plane gap, other tests were also done to note the effect of changing parameters in the geometric model of the rod-plane gap. An analysis of these tests is given in *Appendix D*. The parameters that were varied in the tests were :

- Changing the value of s which defines the position at which the space charge, Q_s is placed in the gap
- Varying the magnitude of the space charge, Q_s
- Adjusting the radius of the sphere used to model the space charge, Q_s

The results from the above tests are as follows :

- Doubling the value of s causes the induced voltage to drop from 558.48kV to 558.44kV which can be regarded as having a negligible effect.
- Changing the space charge magnitude by three orders of magnitude makes no difference
- Changing the space charge radius by a factor of ten makes no significant difference

4. The Conductor-Plane Gap

The procedure for determining the continuous leader inception voltage for the conductor-plane gap is the same as that for the rod-plane gap. However, the geometric configuration of the conductor-plane gap is not as simplified as that for the rod-plane gap and this is accounted for in the model by the amount of charge that is induced on the high voltage electrode. In the rod-plane gap the potential, U'_{ge} that is measured largely consists of induced voltage due to the image charges of Q_e since the charge induced on the rod is negligible as a result of the rod having such a small surface area. However, in the case of the conductor which has a far greater surface area than the rod, primarily due to its length parallel to the plane, the measured potential, U'_{ge} is to a large extent influenced by the induced charge on the conductor.

The calculation for the leader voltage drop is more complicated than that for the rod-plane gap as the leader length, l_e, is dependant on the leader gradient, E_e and the conductor radius, a, as is discussed in *Appendix B.3.2*.

4.1 The Continuous Leader Inception Voltage

4.1.1 Model for the Conductor-Plane Gap

The formula for the continuous leader inception voltage is given by *equation B.10* where the unknown value of R is again determined by a charge simulation technique as is described in *Appendix B.2*. The parameter, U'_{ge} has been determined empirically by Rizk [Rizk Oct. 1989] to be 2247kV. The value of A is a function of the way in which the model for the conductor-type geometry is defined and is indirectly dependant on the value of R when using the charge simulation technique. This is discussed below in greater detail.

An analytical expression for the magnitude of R in a conductor-plane gap has been derived by Rizk [Rizk Oct. 1989] using Bessel functions. The expression for R shown in

equation 4.1 is a function of the gap distance, d, the conductor radius, a, and the position of the space charge with respect to the high voltage electrode, s.

$$R = \frac{2d \ln \frac{2d}{a}}{\ln \frac{s}{a}} \tag{4.1}$$

Inserting *equation 4.1* into *equation B.10*, the expression for the continuous leader inception voltage becomes :

$$U_k = \frac{U_{cc}}{1 + \frac{B(a)}{d \ln \frac{2d}{a}}} \tag{4.2}$$

where the expression for $B(a)$ is :

$$B(a) = 0.54 \ln \frac{s}{a} \tag{4.3}$$

Rizk makes use of *equation 4.2* and empirical data from his previous work [Rizk Jan.1989] to obtain an analytical expression for the continuous leader inception voltage shown in *equation 4.4*.

$$U_k = \frac{2247}{1 + \frac{5.15 - 5.49 \ln a}{d \ln \frac{2d}{a}}} \tag{4.4}$$

Equation 4.3 has been tested and corresponds well with practical results but in order to adopt a charge simulation technique, the format of *equation B.10* still needs to be used where a value of A is known so that the continuous leader inception voltage can be calculated for any value of R. By equating *equation 4.2* with *equation 4.4* the following expression is obtained :

$$0.5A \ln \frac{s}{a} = 5.15 - 5.49 \ln a$$

and making A the subject of the formula :

$$A = \frac{10.3 - 10.98 \ln a}{\ln s - \ln a} \tag{4.5}$$

Thus in order to solve for the continuous leader inception voltage in conductor-type geometry's by adopting a charge simulation technique, the following procedure must be followed :

- Determine a value for R using a charge simulation technique
- From *equation 4.1* for a known gap distance, d, and conductor radius, a, determine an effective value for s which is not necessarily the same magnitude as s chosen for the charge simulation technique
- Calculate a value of A from *equation 4.5* using the effective value of s and the known conductor radius, a
- Determine the value of the continuous leader inception voltage, U_i, using *equation B.10*

A 2D model of the charge simulation technique been used for the conductor-plane gap is shown in *Figure B.2*.

It should be noted that the effective value of s determined as mentioned above can only be meaningful if the chosen value of s where the space charge is placed falls within a safe region - Rizk has specified that when deriving his analytical expression for R shown in *equation 4.1* it was necessary to specify that the position, s, at which the space charge is placed is much greater than the conductor radius, a, in order to neglect the effect of harmonic charge distribution on the conductor. To ensure that spatial harmonic effects do not interfere with the solution, s must always be defined to be greater then a. It is also a specification of the model that the position of the space charge is much smaller than the

gap distance, d. This prerequisite of the model also makes sense when it is considered that the transition from the streamer-stem to the leader-stem occurs at a position close to the high voltage electrode which is much smaller than the gap distance. Thus when defining the model for the conductor-plane gap, two conditions are satisfied, the first being $s >> a$ and the second being $s << d$. If s is defined to be much smaller than the gap distance, then the exact position of the space charge or magnitude of s is not important. This is verified in *Appendix D.2.1*.

An alternative approach to the method described in this section can be used for calculating a value of A. Once a value for R has been obtained using a charge simulation technique, a value for A in *equation B.10* can be calculated by working back using a known value for the continuous leader inception voltage for a particular geometry which can be obtained from measured results. A large database of breakdown voltages from which the continuous leader inception voltage can be calculated is required if this approach is to be adopted as the value of A varies with gap distance and is also unique for a specific geometrical configuration. This is a main disadvantage of using this approach and it becomes impractical when more complex electrode configurations are examined for which measured values are harder to find.

4.1.2 Prediction of Leader Inception Voltage

4.1.2.1 A 2m Conductor-Plane Gap

When defining the model for the conductor-plane gap, an 80m copper conductor with a radius of 10mm was used. The reason for using such a long conductor was so that the conductor length would be much greater than the gap distance in order to limit the influence of edge effects from the conductor. The gap length between the base of the conductor and the ground plane was 2m. The space charge had a radius of 1mm and was placed at a distance of 200mm from the base of the conductor. Hence, the position of s was at least 10 times greater than the conductor radius and 10 times smaller than the gap length. A charge of 5μC was used for the space charge. The total induced voltage was measured at a distance 80mm from the space charge or 1880mm above the ground plane. In order to speed up computation time, 2400 elements were used in the simulation. Using

a smaller number of elements reduces the accuracy of the output. However, when comparing the results between using in the order of 2500 elements and 8000 elements, there was found to be little difference and indeed insufficient difference to jeopardise the results.

The results for the total induced voltage in the 2m conductor-plane gap are listed in *Appendix C.1.3* and plotted in *Figure 4.1* with respect to height above the ground.

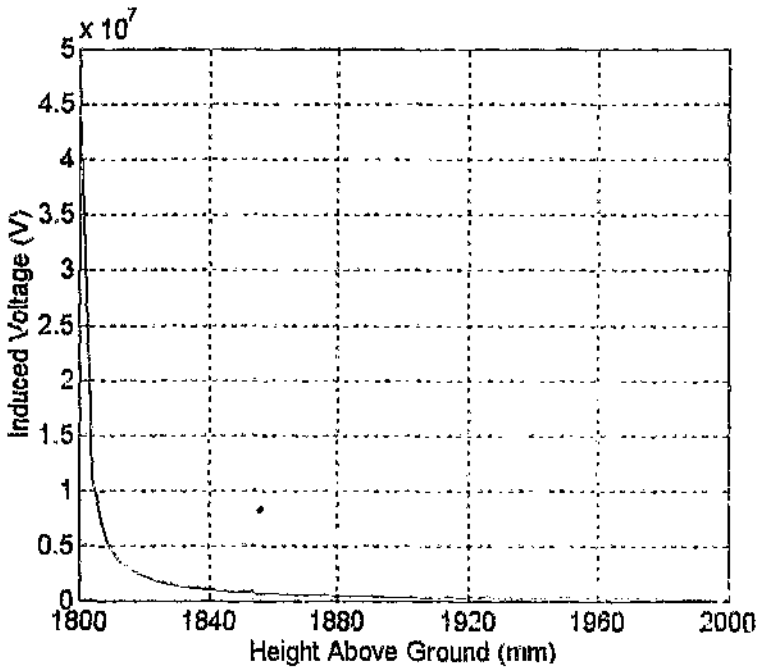

Figure 4.1 - Total Induced Voltage for the 2m Conductor-Plane Gap

The total induced voltage, U_m, measured at a point P, which is 80mm from the centre of the space charge, is 508.5kV. Substituting for U_m, Q_m s and s_m into *equation B.8*, the value of R is evaluated as 0.8406m. From *equation 4.1*, the effective value of s is calculated which when substituted into *equation 4.5* results in a value of A equal to 2.12. The magnitude of the continuous leader inception voltage is then calculated from *equation B.10* to be 638.0kV.

It is appropriate to mention at this point that although a large value of R is obtained for the rod-plane gap, this is not the case for the conductor-plane gap. The reason for this is that the induced potential, U_{ip}, due to the image charges of the space charge and any charge induced on the conductor, is dominated by the charge induced on the conductor because of the large conductor surface area. The component of U_{ip} corresponding to the image charge, $-Q_o$, and charges induced on the image conductor is very small when measured at the point P. However, the component of U_{ip} due to charge induced on the conductor is large due to its close proximity to the measuring point P and hence when summing the two components of U_{ip}, the resultant value of U_{ip} is large and thus R is small.

4.1.2.2 A 6m Conductor-Plane Gap

In the test on the 6m conductor-plane gap, the same dimensions were used as for the 2m conductor-plane gap with the exception of the gap length being increased to 6m.

The results of the test for the total induced voltage can be found in *Appendix C.1.4* and are plotted in *Figure 4.2*.

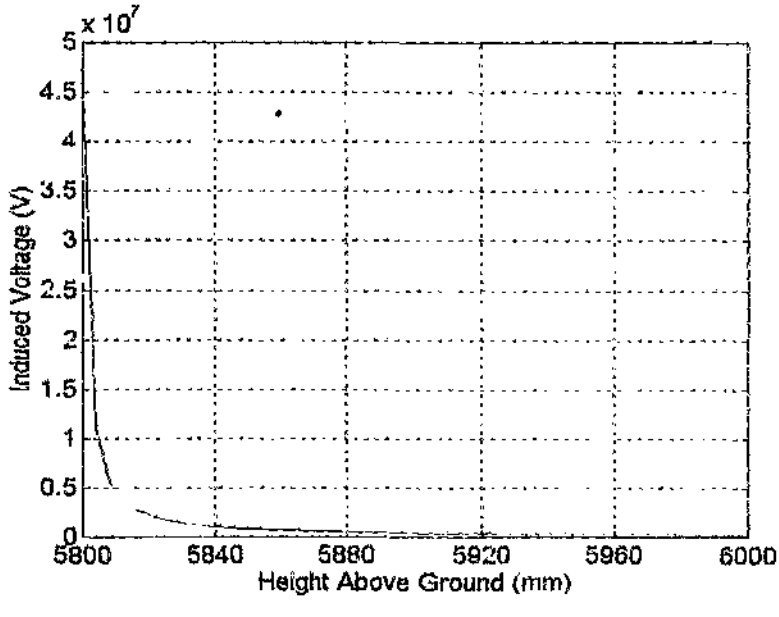

Figure 4.2 - Total Induced Voltage for the 6m Conductor-Plane Gap

The total induced voltage, U_p, measured at a point P, 80mm from the centre of the space charge, is 511.4kV. Substituting for the necessary parameters in *equation B.8*, the value of R is calculated to be 0.8889m. Using *equation 4.1* to determine an effective value of s from the calculated value of R, the given gap distance, d, and the conductor radius, a, and then substituting for this value of s into *equation 4.5*, a value of A equal to 0.6233 is obtained. The value of the continuous leader inception voltage is then determined from *equation B.10* to be 1321kV.

4.2 The Leader Voltage Drop

The leader voltage drop can be calculated for any leader length, l_L, by using *equation B.16*. In order to evaluate the leader length, the height of the final jump needs to be known which in turn is dependant on the leader gradient, E_L. An approximate value for the leader gradient can be obtained using *equation B.20*.

Substituting the necessary parameters given in *Appendix B.3.2* into *equation B.20*, the leader gradient for a 2m conductor-plane gap with a conductor radius of 16mm is calculated to be 197.9kV/m. The height of the final jump is calculated from *equation B.21* to be 1.654m. Hence, with the leader length being the difference between the gap length and the height of the final jump, the leader length is calculated as 0.346m. From *equation B.16* the leader voltage drop for a 2m conductor-plane gap is evaluated to be 65.15kV.

For a 6m conductor-plane gap, the leader gradient is calculated from *equation B.20* to be 233.5kV/m. Thus, the height of the final jump is, using *equation B.21*, equal to 3.462m and therefore the leader length is 2.538m. The leader voltage drop for a 6m conductor-plane gap is evaluated from *equation B.16* to be 203.7kV.

4.3 The Breakdown Voltage

The minimum breakdown voltage, U_B, is obtained as the sum of the continuous leader inception voltage and the leader voltage drop.

$\Rightarrow$ 2m Conductor-Plane Gap : $U_g = U_k + \Delta U_i = 638.0\text{kV} + 65.15\text{kV}$
$= 703.1\text{kV}$

$\Rightarrow$ 6m Conductor-Plane Gap : $U_g = U_k + \Delta U_i = 1321\text{kV} + 203.7\text{kV}$
$= 1525\text{kV}$

The 50% breakdown voltage, U_{50}, is calculated from the minimum breakdown voltage using *equation B.22*. A value of 3% is used for the statistical variation, σ, in conductor-type gaps [Rizk, Oct. 1989]. Thus, substituting values for U_g into *equation B.22* the 50% breakdown values are 772.6kV and 1675kV for the 2m and 6m conductor-plane gaps respectively. These results of the U_{50} values are compared in *Table 4.1* with results measured in practice [Paris] which have been recorded using the critical time to crest waveform for the particular geometry and under dry conditions.

	Predicted, using R	**Measured**	**Percentage difference**
2m Conductor-Plane Gap	772.6kV	840kV	8.7%
6m Conductor-Plane Gap	1675kV	1640kV	2.1%

Table 4.1 - Conductor-Plane Comparison Between Theory and Measured U_{50} Values

Comparison of the theoretical results with those measured in practice shows that the theoretical result is very conservative at 2m but that as the gap length increases to 6m, the measured result has a lower breakdown value. However, the small percentage error for the 6m gap means that the conductor-plane model can be used to determine minimum clearance values using the 50% breakdown voltage and would only need a small safety factor to be included. The reason for such a high percentage difference in the 2m gap is due to the fact that the geometry is far more sensitive to its environment as a result of the two electrodes being so close together. Leader breakdown is thus accompanied by greater errors in the breakdown voltage.

Additional tests on the conductor-plane model have been carried out, the results of which are summarised in *Appendix D*. The following parameters were varied :

- The position, s, of the space charge is changed
- The radius, a, of the conductor is varied
- The single conductor is replaced with a bundle of four conductors

The results of the tests are as follows :

- Changing the position of the space charge within the given specifications ($s >> a$ and $s << d$) has no effect on the breakdown voltage
- Reducing the space charge radius results in a lower breakdown value as a higher gradient would then exist around the conductor
- The charge simulation method provides satisfactory results when modelling a conductor-bundle to plane gap when compared with breakdown values measured in practice

5. The Tower-Conductor Gap

With satisfactory results having been obtained in verifying the charge simulation method for the models of the rod-plane and conductor-plane gaps, the charge simulation method can confidently be used in attempting to verify Rizk's model for conductor-type gaps by examining the tower-conductor window configuration. This is because the tower is regarded as a series of ground planes in the near vicinity of the conductor, that surround the conductor and hence resembles three superimposed conductor-plane configurations. This approximation is satisfactorily verified by the results which show that the influence of non-plane like structures further away from the conductor have negligible effect on the dominant influence of the ground planes surrounding the conductor.

The air gap between the tower and the conductor is an important factor in the design of transmission line towers. The inside or centre phase conductor to tower configuration on a tower is the most important when determining clearance distances in tower design as it has a lower breakdown voltage than the two outside phase conductor to tower configurations [Kachler, LaForest & Zaffanella]. Since the tower window, in which the tower structure completely surrounds the conductor, is the weakest insulation structure [Lloyd & Zaffanella], it is the main focus in this project when attempting to apply Rizk's model to tower-conductor window gaps.

5.1 The Continuous Leader Inception Voltage

5.1.1 Model for the Tower-Conductor Gap

The tower-conductor window configuration can be defined as a conductor-type gap and hence the work of Rizk can be applied in order to determine the breakdown voltage for a specified air gap and electrode geometry. The parameter, U_{cr}, in Rizk's model for the continuous leader inception voltage, U_{50}, defined in *equation B 10* is thus the same as that for the conductor-plane gap which is equal to 2247kV.

The method for determining R by the charge simulation method is the same as that for the rod-plane and conductor-plane gaps. Once a value for R has been calculated, the magnitude of the parameter A which also appears in *equation B.10* is determined using the same method as for the conductor-plane gap which is described in section *4.1.1. Model for the Conductor-Plane Gap.*

The model used to determine the continuous leader inception voltage for the tower-conductor window gap, where the window is a square structure that completely surrounds the conductor, is shown in *Figure 5.1*. It can be seen from *Figure 5.1* that as a result of the conductor, insulator strings and space charge being surrounded by four ground planes, the model becomes rather complex since four groups of images need to be defined. The position of the space charge, Q_o, has also been defined such that a breakdown will occur to a side window, as the results measured in practice that are used to verify the simulation results have been taken for flashovers to the side window.

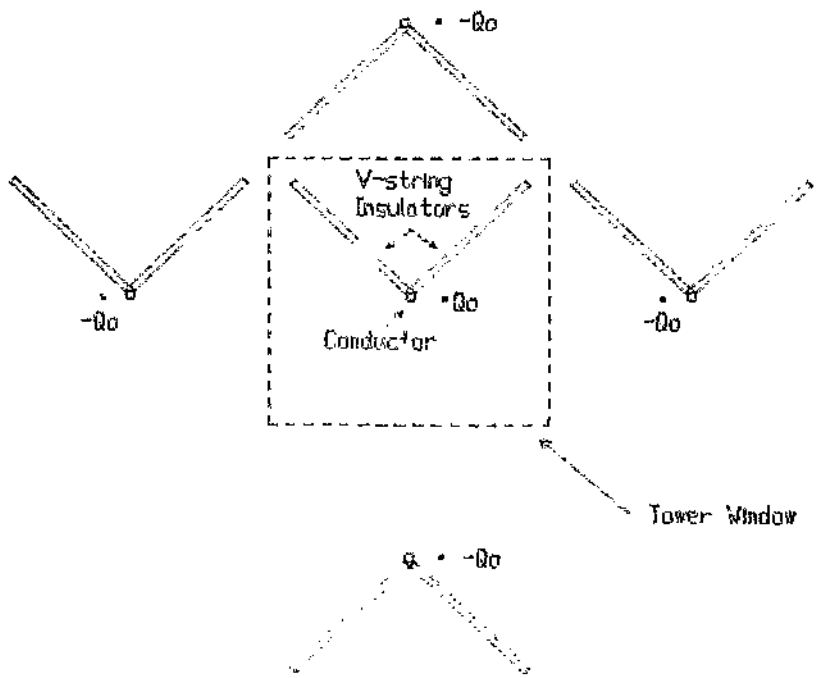

Figure 5.1 - Model for the Tower-Conductor Window Gap

5.1.2 Prediction of Leader Inception Voltage

5.1.2.1 A 5m Tower-Conductor Gap

The model for the tower-conductor gap has an 80m long copper conductor with a radius of 16mm. The gap length between the side of the conductor and any of the four ground planes was 5m. The space charge had a radius of 1mm and was placed at a distance of 200mm from the side of the conductor such that the continuous leader inception voltage for a side flashover could be calculated. A charge of 5μC was used for the space charge which was modelled as a perfect conductor. The conductor is held up by two 6m insulator strings in a V-string setup with an angle of separation between the insulators equal to 90 degrees. It is necessary to define the insulator string length to be at least 1.2 times the gap distance in order to prevent a flashover from occurring along the insulator string [Galet, Leroy, Lacey & Kromer]. The insulator string is modelled as a glass cylinder with a relative permittivity of 5.5 and conductivity of 1e-12S. The glass cylinder has a radius of 127mm and thus adequately represents a combination of the well known 5.75x10 inch insulators used in insulator strings. The total induced voltage was measured at a distance 80mm from the space charge or 4880mm from the side ground plane of the tower window structure. The computation time was reduced by defining 2750 elements in the model.

The results for the total induced voltage, U_m, in the 5m tower-conductor gap are listed in *Appendix C.1.5* and have been plotted as a function of the distance to the side of the tower window structure in *Figure 5.2*.

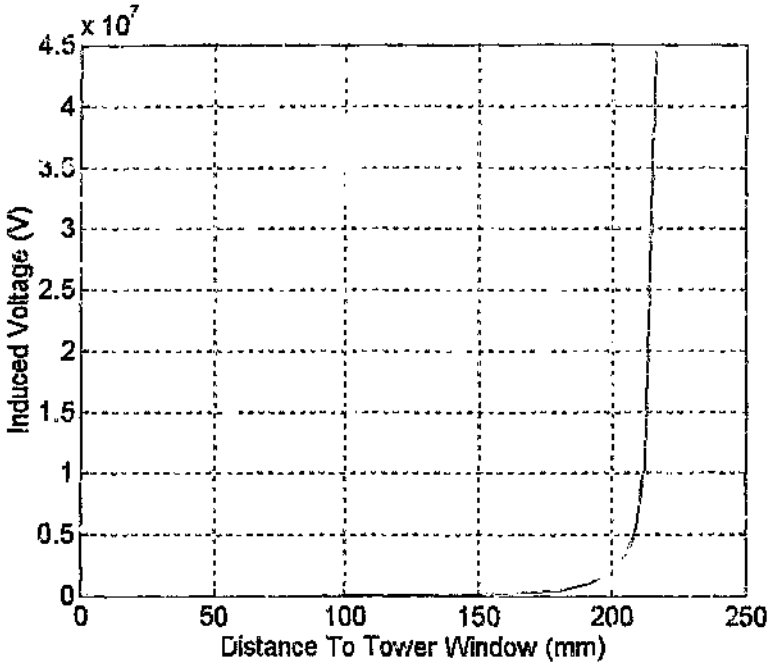

Figure 5.2 - Total Induced Voltage for the 5m Tower-Conductor Gap

If the *Figure 5.2* is compared with any of the figures for the total induced voltage in the rod-plane and conductor plane gaps, it is noticed that the attenuation from the peak voltage to the measuring point, 80mm from the peak voltage, is far more severe for the tower-conductor window gap than for the rod-plane and conductor-plane gaps. This is because the tower-conductor gap has three additional ground planes across which images of the conductor, the space charge and the insulators are modelled and thus accounting for a larger value of the component U_{ib} in the total induced voltage.

Although it is very hard to see from *Figure 5.2*, the total induced voltage 80mm from the centre of the space charge is best obtained from *Appendix C.1.5* and is equal to 105.8kV. Substituting this value for U_{ins}, a value of Q_o equal to 5μC, s equal to 200mm and s_o equal to 120mm into *equation B.8*, the value of R is evaluated as 0.09855m. From *equation 4.1*, the effective value of s is calculated which when substituted into *equation 4.5* results in a value of A equal to 0.08526. The magnitude of the continuous leader inception voltage is then calculated from *equation B.10* to be 1205kV.

The value for R is smaller than that calculated for either the rod-plane or conductor-plane gaps. The reason for this is that the component, U_{ch} of the total induced voltage is far greater in the case of the tower-conductor gap as has been mentioned earlier in this section. As a result of a large value for U_{ch} the magnitude of R is smaller.

5.1.2.2 A 9.3m Tower-Conductor Gap

The geometry for the 9.3m gap is the same as that for the 5m gap with the exception of an increase in the gap length and thus also a corresponding increase in the insulator string length to 11.16m. The total induced voltage was measured at a distance 80mm from the space charge or 9180mm from the side ground plane of the tower window structure. The computation time was once again reduced by defining 2750 elements in the model.

Values for the total induced voltage for the 9.3m gap are listed in *Appendix C.1.6* and plotted in *Figure 5.3* with respect to the distance to the side of the tower window structure.

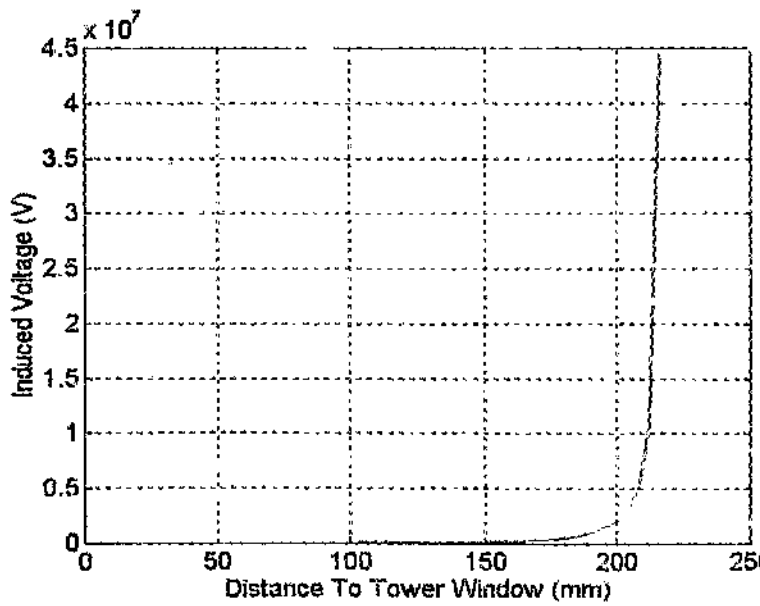

Figure 5.3 - Total Induced Voltage for the 9.3m Tower-Conductor Gap

Using the data in *Appendix C1.6*, the total induced voltage, U_{ind} at a point 80mm from the centre of the space charge is 106.8kV. The magnitude of R is obtained as 0.09878m using *equation B.8* and substituting for U_{ind}, Q_{sc}, s and ε_0. The effective value of s is calculated from *equation 4.1* and when substituted into *equation 4.5* results in a value of A equal to 0.04838. The magnitude of the continuous leader inception voltage is then calculated from *equation B.10* to be 1508kV.

5.2 The Leader Voltage Drop

The method for calculating the leader voltage drop in the tower-conductor gap is the same as that for the conductor-plane gap. Firstly, the leader gradient, E_l, needs to be determined from *equation B.20* for a given conductor radius, a, and gap length, d. The leader gradient is then used to determine the height of the final jump, h_j, from *equation 21* from which the leader length, l_l, is obtained as the difference between the gap length and the height of the final jump. Finally, the leader length is used in conjunction with *equation B.16* to compute the leader voltage drop.

For the 5m tower-conductor gap with a 16mm conductor radius, the leader gradient is obtained as 235.4kV/m. The height of the final jump is then evaluated as 3.134m and thus the leader length is 1.866m. The leader voltage drop is calculated to be 168.4kV.

The leader gradient for the 9.3m tower-conductor gap is computed to be 212.6kV/m. This gives a value for the height of the final jump equal to 4.195m which corresponds to a leader length of 5.105m. The leader voltage drop is then calculated to be 555.0kV.

5.3 The Breakdown Voltage

The minimum breakdown voltage, U_b, for the 5m and 9.3m tower-conductor gaps is calculated by summing the continuous leader inception voltage and the leader voltage drop :

$\Rightarrow$ 5m Tower-Conductor Gap : $U_B = U_K + \Delta U_i$ = 1205kV + 168.4kV
= 1373kV

$\Rightarrow$ 9.3m Tower-Conductor Gap : $U_B = U_K + \Delta U_i$ = 1508kV + 555.0kV
= 2063kV

The 50% breakdown voltage is calculated from the minimum breakdown voltage using *equation B.22* with a statistical variation, σ, equal to 3% [Rizk, Oct. 1989]. Thus the 50% breakdown voltages are calculated to be 1509kV and 2267kV for the 5m and 9.3m tower-conductor gaps respectively. These results for the U_{50} are compared with results measured in practice [Lloyd & Zaffanella] for square tower windows in *Table 5.1*. The results have been recorded with test conditions using critical time-to-crest waves and under standard atmospheric conditions.

	Predicted, using R	**Measured**	**Percentage difference**
5m Tower-Conductor Gap	1509kV	1590kV	5%
9.3m Tower-Conductor Gap	2267kV	2180kV	3.84%

Table 5.1 - Tower-Conductor Comparison Between Theory and Measured U_{50} Values

The percentage error between theoretical results and those measured in practice is greater in the case of the tower-conductor gap than for the rod-plane or conductor-plane gaps. Like for the conductor-plane gap, the results produced by the model are conservative for smaller air gaps such as is the case with the 5m tower-conductor gap. However, for larger 9.3m air gap, the measured value for the 50% breakdown voltage is lower than that predicted.

Thus, even though the percentage errors are relatively small which consequently verifies that the model produced by Rizk can be applied in calculating minimum clearance distances for the design of transmission line towers, corrective measures of a few percent should be applied as a safety factor where large air gaps greater than 5m are concerned.

There is no need to include a safety factor for tower-conductor air gaps less than 5m in length as the breakdown values predicted using the model of Rizk are already conservative.

Further tests which have been carried out on the tower-conductor configuration are :

- A test where the tower window structure contains three sides - a top and two side ground planes - in a square setup
- The single conductor is replaced by a bundle of four conductors. The tower window structure contains three planes in a square setup

The results of these tests are discussed in *Appendix D* and summarised as follows :

- The charge simulation technique is suitable for modelling tower window structures with three side planes in a square setup and provides conservative values for the breakdown voltage
- Tower-conductor-bundle gaps can be modelled using the charge simulation technique although a small safety factor needs to be included when calculating the minimum clearance distances as the measured values for breakdown are slightly conservative with respect to the breakdown values obtained using the charge simulation technique

6. Summary and Recommendations

6.1 Summary

The Rizk model has been tested using a charge simulation technique to verify the positive switching impulse breakdown voltage for a rod-plane and conductor-plane gap. With satisfactory results having been achieved using the *Coulomb* charge simulation package, the model was applied to a conductor-type gap in the hope that the breakdown voltage for a tower-conductor window gap, subjected to positive switching impulses stresses, could be determined. The results from the simulation discussed in *Chapter 5* verify that confident values for the 50% breakdown voltage in the tower-conductor configuration can be obtained by applying the Rizk model.

In the rod-plane gap, the percentage error between the simulation results using the Rizk model with a refined value for R and the measured results in practice, for 50% breakdown voltage in the 3m and 7m gaps, was 0.946% and 3.8% respectively. The percentage error increases with gap length. However, both of the breakdown voltages obtained from the simulation are lower than and hence conservative with respect to the measured values. There is very little difference between the Rizk model when using a value of R equal to $2d$ and using a refined value for R, but the charge simulation technique is more appropriate in that more conservative and thus safer values for the breakdown voltage are obtained.

The percentage error for the conductor-plane gap also decreases with gap length. In the 2m gap the error is 8% whilst for the 6m gap it is 2.1%. Contrary to the rod-plane gap, only the breakdown voltage for the 2m gap is conservative whereas the 6m gap has a breakdown voltage that is slightly higher than that measured in practice. Thus, it can be concluded that where the Rizk model is used for designing clearance distances for the conductor-plane gap where the gap length is larger than 2m, a safety factor should be included.

The tower-conductor gap, being a conductor-type gap, has similar characteristics to the model for the conductor-plane gap. The percentage error decreases with gap length. The 5m gap has an error of 5.09% whilst the 9.3m gap has a percentage error of 3.8%. Like for the conductor-plane gap, the breakdown voltage at the lower gap length is conservative with respect to the measured result, whereas for the larger gap length, the breakdown voltage obtained through simulation is slightly larger than that measured in practice. Once again, this calls for the inclusion of a safety factor when using the model to calculate clearance distances in the design of tower-conductor gaps.

Conclusions which can be drawn from additional tests done on the rod-plane, conductor-plane and tower-conductor gaps are mentioned below.

In the rod-plane gap, increasing the distance at which the space charge is placed from the rod tip reduces the accuracy of the charge simulation method. A change of the space charge magnitude has no effect on the overall results as the image charges are also scaled which results in a zero net overall effect. Changing the radius of the space charge also has no effect on the 50% breakdown voltage calculated when using the charge simulation method.

In the conductor-plane gap, changing the position of the space charge has no effect on the 50% breakdown voltage. Reducing the conductor radius results in a larger E-field gradient around the conductor relative to a conductor with a larger radius. Consequently, leader inception and breakdown occur at a lower voltage. The conductor-plane model of Rizk can be used to model conductor-bundle to plane configurations producing results which are conservative with respect to flashover values measured in practice.

The tower-conductor gap was examined where the tower window structure only had three planes at ground potential - two side planes and a top plane. Results from the charge simulation method verified once more that Rizk's model is suitable when determining the positive switching impulse breakdown voltage for tower-conductor gaps. A test which investigated whether the Rizk model can be applied to tower-conductor-bundle configurations proved to be successful although a small safety factor would need to be

incorporated so that the theoretical breakdown voltage would be conservative relative to the breakdown voltage measured in practice.

6.2 Recommendations

The model of Rizk has been tested for rod-plane and conductor-plane gaps and applied to tower-conductor gaps with satisfactory results. However, the model can be extended and used in areas which may be the focus of further research in the future. Some ideas are mentioned below :

In addition to the tower window structures tested, further research should use tower window structures more applicable to that currently being used or studied for future use.

The model of Rizk should be studied to include the effects of variations in atmospheric conditions.

Rizk's model should be tested using a charge simulation technique where the model can be applied to determine the phase to phase breakdown voltage. Analytical work by Rizk already exists in this field, but the model should be verified using an appropriate simulation technique so that it can be applied to other structural and gap configurations as has been done in this research.

There is also a need to include the effects of floating objects. Like with phase to phase breakdown as discussed above, a model by Rizk also exists to include floating objects. However, the model has not been tested and applied to alternative geometry's whilst using a charge simulation package.

Finally, the model by Rizk which has been studied in this research defines an analytical expression for the value R in conductor-plane gaps. This expression has been obtained using Bessel functions but is unique to single conductors above a plane. In order to apply Rizk's model so that conductor-bundle plane or tower-conductor-bundle configurations

can be studied accurately, an analytical expression for a conductor-bundle above a plane should be derived from which the value of R can be calculated.

Acknowledgements

I would like to thank the following people for their kind assistance with this research :

Prof. J.P.Reynders, my supervisor, who guided me through each stage of the research and assisted in defining a realistic goal for the research work.

Dr. L. van der Zel, who organised the *Coulomb* package on behalf of ESCOM, without which this research project would never have been possible.

Dr. J. van Coller for his assistance in analysing the work of Rizk.

Dr. A. Phillips who suggested the model of Rizk and gave recommendations to alternative models which could be studied in determining the breakdown voltage due to switching impulses.

References

Aihara, et al., "Impulse flashover characteristics of long air gaps and atmospheric correction," *IEEE Transactions on Power Apparatus and Systems*, Vol. PAS-97, pp.342-348, March/April 1978

Ansoft, *Maxwell 2D and 3D Field Simulator V. 6.4.16, Control Panel V.1.7.66*, Ansoft Corporation, 1996

Berger, et al., "L'Amorcage Dans L'Air Aux Grandes Distances," (UHV Networks : Determination of insulation distances), *RGE*, Special issue, pp.763-787, June 1974

Carrara, G. and Thione, L., "Switching surge strength of large air gaps : A physical approach," *IEEE Transactions on Power Apparatus and Systems*, Vol. PAS-95, no.2, pp.512-524, March/April 1976

Dillard, J.K. and Hileman, A.R., "UHV transmission tower insulation tests," *IEEE Transactions on Power Apparatus and Systems*, Vol. PAS-89, no.8, pp.1772-1784, November/December 1970

Gallet, G., Leroy, G., Lacey, R. and Kromer, I., "General expression for positive switching impulse strength valid up to extra long air gaps," *IEEE Transactions on Power Apparatus and Systems*, Vol. PAS-94, no. 6, pp.1989-1993, November/ December 1975

Gallimberti, I., "The mechanism of the long spark formation," *Journal de Physique*, Colloque C7, supplement au no. 7, Tome 40, pp.225-226, Juillet 1979

Harada, T., Aihara, Y. and Aoshima, Y., "Influence on switching impulse waveshape on flashover voltage of air gaps," *IEEE Transactions on Power Apparatus and Systems*, Vol. PAS-92, no. 3, pp.1085-1093, May/June 1973

Hochrainer, A., "Einige Bemerkungen zum Stromnulldurchgang in Wechselstromschaltern," *EuM*, Vol. 87, no. 1, pp.15-19, 1970

I.E.S., *Coulomb - Three Dimensional Electric Field Solver V. 2.1. Users and Technical Manual*, Integrated Engineering Software Incorporated, 1989

Jones, B., "Switching surges and air insulation," *Phil. Trans. R. Soc. Lond.*, A. 175, pp.165-180, 1973

Kachler, A.J., LaForest, J.J., Zaffanella, L.E., "Switching surge flashover of UHV transmission line insulation," *IEEE Summer Power Meeting and EHV Conference*, pp.1604-1611, July 12-17 1970

Kuffel, E. and Zaengl, W.S., *High Voltage Engineering Fundamentals*, pp.377-378, Pergamon Press, 1984

Lloyd, K.J., Zaffanella, L.E., "Insulation for switching surges," *Transmission Line Reference Book : 345kV and Above*, Chapter 11, pp.503-544, 2nd Edition, Electric Power Research Institute, Palo Alto, CA., 1987

Niemeyer, L., Ullrich, L., Wiegart, N., "The mechanism of leader breakdown in electronegative gases," *IEEE Transactions on Electrical Insulation*, Vol. 24, No. 2, pp.309-324, April 1989

Paris, L., "Influence of air gap characteristics on line-to-ground switching surge strength," *IEEE Transactions on Power Apparatus and Systems*, Vol. PAS-86, no.8, pp.936-947, August 1967

Rizk, F.A.M., "A model for switching impulse leader inception and breakdown of long air-gaps," *IEEE Transactions on Power Delivery*, Vol. 4, no.1, pp.596-606, January 1989

Rizk, F.A.M., "Switching impulse strength of air insulation : leader inception criterion," *IEEE Transactions on Power Delivery*, Vol. 4, no.4, pp.2187-2195, October 1989

Sadurski, K.J., Van Der Merwe, C.W., Muftic, Dz., "Live line maintenance of EHV and UHV transmission lines - factors influencing the dielectric strength at the work site," *Cigre*, 33-304, 28 August-3 September 1994

Appendix A

The literature survey listed in this appendix covers several aspects of the breakdown process involved with switching impulses. These aspects mainly involve the streamer inception criterion, breakdown for long air gaps and the inclusion of floating objects. Models proposed by various researchers and the work of academics are listed for each researcher together with any problems and assumptions. Papers which deal with experimental work and which produce graphical results but which do not describe any particular model or lead to any analytical expression for calculating the switching impulse voltage have been read but not included in this summary. They are available should they be needed to verify or analyse results obtained by a particular model.

The authors and the available knowledge is as follows :

Kuffel and Zaengl

Article 2 :

- Provides a correction for the variation in the ambient conditions by introducing the relative air density, δ, which is multiplied by the breakdown voltage at standard conditions to give the corrected breakdown voltage. The correction factor, δ, is :

$$\delta = 0.386 \frac{p}{273 + t} \tag{A.1}$$

with p = atmospheric pressure (Torr)

t = temperature (°C)

- States that the condition for discharge inception and possible breakdown in a non-uniform gap is given by the following relation :

$$\int_0^d \alpha - \eta dx = N_{cr} \tag{A.2}$$

where x = the path of the avalanche when the streamer is initiated

d = the gap length

α and η = the ionisation and attachment coefficients respectively

N_{cr} = 18-20 for the streamer criterion

There is a transition from the Townsend criterion (N_{cr} = 8-10) for sparking to the streamer criterion which is dependant on the pressure, p, and the gap spacing, d. This transition occurs when the product $pd \geq$ 1-2 bar.cm. Thus, for large gaps and in non-uniform conditions it is understood that the above relation applies and that the breakdown voltage or corona inception voltage, depending on which one occurs, can be calculated if after a certain distance, x, the above relation holds.

- The special case of corona inception in a coaxial cable is considered and the analytical expression for calculating the corona inception voltage is :

$$\left(\frac{E_c}{\delta}\right)^2 - 2\left(\frac{E_c}{\delta}\right)E_c \ln\left[\frac{1}{E_c}\left(\frac{E_c}{\delta}\right)\right] - E_c^2 = \frac{K^2 C}{(\delta r)} \qquad \text{(A.3)}$$

where E_c = the critical field strength

δ = relative air density

r = radius of inner conductor of coaxial cable

K^2C = 42 (kV/cm)^2

This expression provides an improvement over the work of Peek who produced an empirical expression on cables with a small radius where $\delta r \approx 1$.

- States that the critical breakdown strength of air is 26.6kV/cm under standard conditions where temperature = 20°C, air pressure = 101.3kPa and humidity = 11g/m^3

- For positive electrodes, streamers occur when the air is stressed and their size is proportional to the voltage applied such that for a high enough voltage, they will be large enough to cross the gap and lead to breakdown. For small gaps, breakdown normally occurs by the Townsend mechanism before the streamers develop. For large gaps, streamers develop and lead to glow corona after which breakdown follows

With negative electrodes, regular pulses known as Trichel pulses occur when the air is stressed. An increase in voltage or in the pressure leads to an increase in the pulse frequency. Ay higher voltages, glow discharge occurs and then breakdown.

The positive breakdown voltage is lower than the negative breakdown voltage except at low pressures. Hence, for A.C., breakdown occurs on the positive half cycle For impulses, the positive impulse normally has the lower breakdown voltage.

Heymann

Article 12 :

- Here Heymann explains the affect of humidity on the ionisation process As the water vapour content of the air increases, the effect of attachment increase is greater than that of ionisation and consequently the value of E/p at which ionisation equals attachment also increases.

- States that the critical field strength of air is 2.4 MV/m at a pressure of 760 Torr.

- Provides an empirical relation for the field strength, E_a at the wire surface at which ac corona is initiated for concentric and parallel wire arrangements, as follows :

$$\frac{E_a}{\delta} = 2.4 \pm 0.33 + 0.225(a\delta)^{-0.5} \; MV/m \qquad \text{(A.4)}$$

where δ = relative air pressure (to 760 Torr)

a = wire radius (metres)

This empirical formula from Heymann has assumed, from an average of measurements by various authors, that the total exponent in the electron multiplication factor, M, has a value of seven for corona inception

Article 11 :

- Heymann produces a formula for calculating the corona inception voltage for multiple wire bundles. The formula uses the knowledge that the effective field strength (where the corona threshold occurs) is found at a point on the wire surface halfway between the points of greatest and average field strengths - this has been found experimentally. The ratio between the effective field strength, E_e, and the average field strength, E_{av}, for an n wire bundle is given as :

$$\frac{E_e}{E_{av}} = 1 + 0.71(n-1)\frac{d}{b} \tag{A.5}$$

where n = number of wires in the bundle

d = wire diameter

b = diameter of the bundle

This ratio is then used to calculate the rms corona threshold voltage, V_{sc}, which for a two wire bundle is given as :

$$\sqrt{2}V_{sc} = \frac{\frac{E_c d}{2}\left[2\ln\left(\frac{2S}{d}\right) - \ln\left(\frac{b}{d}\right) - \ln 2\right]}{\left(1 + 0.71\frac{d}{b}\right)} \tag{A.6}$$

where S = the separation between the bundles on a transmission line

The rms corona threshold voltage can also be determined for multiple wire bundles.

The maximum corona threshold voltage is found by differentiating the rms voltage equation and also finding the optimum wire spacing. This procedure can be followed for multiple bundles if necessary but for a two wire bundle the maximum threshold voltage is :

$$V_{sc\,max} = E_c d\left[1.5\log\left(\frac{2S}{d}\right) - 0.88\right] \tag{A.7}$$

The critical field strength is evaluated as that which occurs on a single wire which is quantified by a formula which has been empirically derived and is given by *equation A.4*.

- In addition to the above method of calculating the corona onset, Heymann again states that corona commences when the relation in *equation A.2* is satisfied for N_p equal to a value between 7 and 9 and x is the distance at which α is equal to η.

Peek

Dielectric Phenomenon In High Voltage, F.W. Peek, Second Edition, McGraw-Hill Book Company, 1920 :

- Peek stated that for small gaps there is no corona and a direct spark occurs whereas for bigger gaps corona precedes a spark.

- Peek gives the critical field strengths at which corona inception occurs, E_c , for a variety of configurations. These have been determined experimentally :

$$\text{Coaxial : } E_c = 31\delta(1+\frac{0.308}{\sqrt{\delta r}})\ kV/cm \qquad \text{(A.8)}$$

$$\text{Parallel wires : } E_c = 30\delta(1+\frac{0.301}{\sqrt{\delta r}})\ kV/cm \qquad \text{(A.9)}$$

where δ = the relative air density as defined in *equation A.1*

r = the wire radius (cm)

Equation A.8 correlates well with *equation A.3*, however it deviates and becomes incorrect for large values of radii where $\delta r > 1$. Provides sparking voltage calculation for parallel wires based on the empirical critical field strength as shown in *equation A.9*. Peek also gives the corona critical voltages as they relate specifically to transmission lines.

Dielectric Phenomenon In High Voltage, F.W. Peek, Second Edition, McGraw-Hill Book Company, 1929 :

- Provides critical field strength formula for the single wire case from experimental results which compares favourably with the work from Heymann as given in *equation A.4* :

$$E = \delta(3.0 \pm 0.36 + 0.09(a\delta)^{-0.5} MV/m \qquad (A.10)$$

Discussion

The Townsend mechanism is a process whereby a plasma is formed which would lead to breakdown in uniform fields with small gaps or extremely small gaps for non-uniform fields. The plasma is the result of a number of electron avalanches, each avalanche bigger than the preceding one as a result of secondary electrons released when positive ions from the previous avalanche bombard the cathode, such that the mechanism can be described as self-sustaining. The Townsend mechanism is used to predict the sparking threshold which is concurrently the breakdown voltage for small gaps as mentioned above.

In larger gaps, the streamer mechanism is postulated where the avalanche head is high although not high enough to bridge the gap. Instead, the avalanche head constitutes a significant space charge which causes a considerably higher field than that at the applied electrode. Consequently, ionisation from the avalanche head occurs rapidly to the anode forming a conductive channel. The enhanced field in the tail of the avalanche will lead to a conductive channel to the cathode thus bridging the gap. Thus the streamer mechanism is dependant on the avalanche-produced field.

The integral equation is used to calculate the magnitude of avalanche. For corona inception, the critical number is between 7 and 9 and two unknowns are present, that of the voltage magnitude and that of the distance over which the avalanche has grown before more ionisation's than attachments are occurring. For total breakdown, the work of Zaengl which stated the critical number as being 18-20 has been improved as a result of better measurement techniques and now stands at between 11-12. The integration in this case is taken as being across the whole gap.

Rizk

Article 20 :

- Presents continuous leader inception voltage formula for a rod-plane gap under positive switching impulse conditions. This is done by determining the field at the plane, E_p, as a result of the leader space charge which from electrostatics is simplified by Rizk to :

$$E_p = \frac{q_l}{2\pi\varepsilon_0}\left[\frac{1}{d-l_z}-\frac{1}{d}\right] \qquad (A.11)$$

where q_l = charge injected by the leader into the gap

d = gap spacing

l_z = length of axial distribution of charge from the leader into the gap

An assumption is made that the geometric field plays a minor role in determining the field at the plane due to discharge shielding of the point electrode.

For the continuous leader reaches the position of the final jump, two conditions must be simultaneously fulfilled : the leader corona must be of sufficient length to reach the plane, that is of length $d-l_z=h_l$ and the leader tip potential must be able to cause streamer breakdown which occurs at a gradient of E_s = 400kV/m for low breakdown probabilities. Thus the assumption is made that the continuous leader inception occurs at the point of the final jump where the leader tip potential is $U_k = E_s h_l$.

At the point of the final jump, the critical field at the plane is E_{cr} which is = E_p.

Substituting for E_p and h_l into *equation A.11* the following expression is obtained for the continuous leader inception voltage :

$$U_k = \frac{E_s}{\frac{2\pi\varepsilon_0 E_{cr}}{q_l}+\frac{1}{d}} = \frac{\frac{V_{cr}}{E_{cr}}E_s}{1+\frac{V_{cr}}{E_{cr}}\frac{1}{d}} \qquad (A.12)$$

where $V_a = \frac{q_l}{2\pi\varepsilon_0}$

With these relations Rizk develops the relation between the continuous leader inception voltage and the gap spacing :

$$\frac{E_0}{U_{li}} - \frac{1}{d} = \frac{E_{st}}{V_0} \qquad \text{(A.13)}$$

From experimental work it is seen that the relation between the gap spacing and the inception voltage always renders the L.H.S. of Eq. *A.13* constant at a value of 0.257. From this and the value for E_0 listed above, the leader inception voltage is :

$$U_{li} = \frac{1556}{1 + \frac{3.89}{d}} \qquad \text{(A.14)}$$

- By using the conductance of the leader and integrating the resulting expression for the leader gradient, the leader voltage drop is calculated. An exact expression for this voltage drop is given although it is based on experimental work used to determine the leader length :

$$\Delta U_l = \frac{50d}{1 + \frac{3.89}{d}} + 37.5 \ln\left[8 - 7\exp\left(\frac{-1.33d}{1 + \frac{3.89}{d}}\right)\right] \text{ (kV,m)} \qquad \text{(A.15)}$$

The applied voltage at the instant of the final jump, $U_{li} = \Delta U_l + U_{li}$. The 50% spark-over voltage is calculated as

$$U_{50} = \frac{U_{li}}{1 - 3\sigma} \qquad \text{(A.16)}$$

where the standard deviation amounts to 5%. Thus for the rod-plane gap the 50% sparkover voltage which agrees well with experimental results for 2-25m gaps is :

$$U_{50} = \frac{1830 + 59d}{1 + \frac{3.89}{d}} + 44 \ln\left[8 - 7\exp\left(\frac{-1.33d}{1 + \frac{3.89}{d}}\right)\right] \qquad \text{(A.17)}$$

- Rizk also presents the continuous leader inception voltage for conductor-plane gaps although in a lot less detail and with more assumptions due to a higher geometrical complexity. This is given as :

$$U_{lc} = \frac{2360}{1 + \frac{5.6}{d} - 6.5 \times 10^{-3} \frac{E_l}{\ln\frac{2d}{r}}} \quad \text{(kV,m)} \qquad \text{(A.18)}$$

where E_l = the leader gradient which should be determined by iteration as it depends on the length of the leader

r = the equivalent conductor radius

- Rizk also presents a tool whereby the corona inception voltage is equated to the continuous leader inception voltage in order to determine a critical electrode radius.

Article 9 :

- Rizk presents a new approach to determine the continuous leader inception voltage. The approach uses the fact that the difference between the applied field and the space charge induced field is the critical field where the inception is continuous. The fields are related by an equivalent radius to the voltages. The induced voltage is the difference between the induced potential in the vicinity of the high voltage electrode, U_{ie}, and the induced potential due to image charges, U_{ii}.

$$U_{ie} = \frac{Q_e}{4\pi\varepsilon_0(s - s_0)} \qquad \text{(A.19)}$$

and $$U_{sh} = \frac{Q_s}{4\pi\varepsilon_0 R} \qquad (A.20)$$

where Q_s = space charge

s = distance of space charge from high voltage electrode

s_s = distance of tip of the streamer-stem zone from the high voltage electrode

R = distance of image charge from high voltage electrode which is a function of the gap geometry.

From this and the above-mentioned relation between potentials, the continuous leader inception voltage is presented as :

$$U_{ic} = \frac{U_{ic\infty}}{1 + \frac{A}{R}} \qquad (A.21)$$

where $U_{ic\infty}$ and A are dependant on the high voltage electrode configuration and are independent of the gap spacing and ground electrode geometry. *Equation A.21* is identical to the format of *equation A.14* and shows that the two approaches account for the same phenomenon.

In a rod-plane gap, the effect of induced charge on the rod is neglected due to the rod being thin. The geometry of the rod is then regarded as negligible in influencing the induced charge. Thus in the mirror image of the induced charge (*equation A.20*), only the spacing between the charges Q_s and its reflection $-Q_s$ is accounted for in R. Thus, $R = 2d$, where d is the gap spacing. For a rod-plane gap, the values of $U_{ic\infty}$ and A are by comparison with *equation A.14* 1556kV and 7.78 m respectively.

In a conductor-plane gap, the effect of the induced charge on the high voltage electrode cannot be neglected. *Equation A.19* reflects induced charge in the vicinity of the high voltage electrode whether it is neglected or not. *Equation A.20* best reflects the induced charge as it is the mirror image of the induced charge and thus the value of R will vary so

as to account for the geometry on which the charge is induced. Rizk develops an equation for R to include the effect of the high voltage geometry and *equation A.21* with the value of R substituted becomes :

$$U_k = \frac{U_{cc}}{1 + \frac{A \ln \frac{s}{a}}{2d \ln \frac{2d}{a}}} \qquad (A.22)$$

where a = the radius of the conductor

Rizk then compares *equation A.22* to a modified form of *equation A.18* and manipulates *equation A.22* to become :

$$U_k = \frac{2247}{1 + \frac{5.15 - 5.49 \ln a}{d \ln \frac{2d}{a}}} \qquad (A.23)$$

Thus, for a conductor-plane configuration the value of U_{cc} is 2247. The exact value of A is unknown but the ratio of A to R is known as is given in *equation A.23*.

Knowing the values of U_{cc} and A for the rod-plane and conductor-plane configurations, *equation A.21* can then be applied to modified configurations where the value of R is either determined by charge simulation technique or by analytical means.

For a rod-rod configuration, the continuous inception voltage is :

$$U_k = \frac{1556}{1 + \frac{7.78}{R}} \qquad (A.24)$$

where R is then determined by a charge simulation technique also described in this article by Rizk. If the analytical technique is used, then R is replaced by $2(d+h)$ where d is the

gap length and h the height of the ground rod. In this case, the image charge induced on the ground rod is neglected and hence the normal rod-plane constants apply.

For a conductor-rod configuration the image charge on the ground rod can again be neglected (for d ≥ 4m and h ≤ 2d) and thus the known constant and ratio for the conductor-plane configuration can be used. Hence, the continuous inception voltage is :

$$U_k = \frac{2247}{1 + \frac{5.15 - 5.49\ln a}{(d+h)\ln\frac{2(d+h)}{a}}} \qquad \text{(A.25)}$$

which is an analytical approach. The approach to find R by charge simulation can be used but this causes a problem as no expression is given relating R on its own to the continuous leader inception voltage.

Rizk also presents the continuous leader inception voltage for a conductor-cylindrical structure gap.

- In a rod-rod and conductor-rod configuration, the value for E_0, the streamer gradient is taken as 500kV/m.

Article 32 :

- Rizk presents the leader inception criterion for phase to phase configurations. The criterion is similar to that presented in article 9 with slight modifications to account for the phase to phase configuration. One phase has a positive switching impulse, U_{+}, whilst the other has a negative switching impulse, U_{-}. Both impulses have synchronised peaks and critical fronts. The positive leader inception voltage, U_{k+}, is :

$$U_{k+} = \frac{U_{+}}{\left(\beta_1 k + \beta_2\right)\left[1 + \frac{A}{R_{+}} + 0.25\left(\frac{\beta_1 k + \beta_2}{\beta_1 k + \beta_2}\right)^2 \frac{A}{R_{+}}\right]} \qquad \text{(A.26)}$$

where $U_{c,e}$ and A are again dependant on the high voltage electrode configuration and are independent of gap spacing and ground electrode geometry.

β_1 and β_2 are geometrical factors relating U_n and U_p to the applied voltage, U_{appl}, where $U_{appl} = \beta_1 U_n + \beta_2 U_p$

k is a constant relating U_n and U_p where $U_n = k U_p$

R_p and R_n are geometrical functions which can be determined either analytically or by charge simulation techniques.

For a rod-rod configuration, article 9 verified that $U_{c,e}$ = 1556kV, A = 7.78m, and $R_p = 2h$ where h is the rod-plane gap distance. Using this and an approximation for A/R_n and β_2 = 1, the leader inception voltage for a rod-rod configuration is given as :

$$U_{lp} = \frac{1556}{\left\{(\beta_1 k+1)\left[1+\frac{389}{h}+1.95\left(\frac{k+\beta_1}{\beta_1 k+1}\right)^2\left(\frac{1}{d}-\frac{1}{\sqrt{d^2+4h^2}}\right)\right]\right\}} \quad \text{(kV, m)} \quad \text{(A.27)}$$

β_1 varies with gap length and the ratio between the height above ground and gap length. Certain values are given which are experimentally determined.

Similarly for a conductor-conductor configuration, certain approximations are made and a complex expression for the inception voltage is provided which is not listed here but which is given in the available article.

With the leader inception voltage known, the leader voltage drop, ΔU_l, can be evaluated as presented in article 20 (article 20 specifically works with the rod-plane configuration but any configuration can be applied if the leader length is known which is also given by Rizk for the various configurations in these articles). The 50% breakdown voltage for a phase to phase configuration is then given by :

$$(U_c + U_n)_{50} = \frac{(1+k)U_{lp} + \Delta U_l}{1-3\sigma} \quad \text{(A.28)}$$

where σ = 5% for rod-rod and 3%-5% for conductor-conductor configurations.

- The article then presents computer and experimental results for the rod-rod and conductor-conductor configurations.

- Rizk also presents air density corrections for the continuous leader inception voltages and is accounted for in the phase to ground and phase to phase leader inception *equations A.21* and *A.26* respectively by replacing A with A/δ where δ is the relative air density given in *equation A.1*. With air density correction the leader length and hence leader voltage drop is corrected and thus also the 50% breakdown voltage. These corrections on leader length are shown by Rizk.

Article 3 :

- In this article, Rizk addresses the problem of floating objects and their influence on the insulating strength of phase to ground gaps subjected to positive switching impulses. A model is presented with a floating sphere in a rod-plane gap configuration. The sphere has a small protrusion which simulates a practical situation where the floating object is not perfectly smooth. Furthermore, by corona discharge from the protrusion, the accumulation of free charge on the sphere is inhibited.

Streamer or positive leader breakdown is possible for positive switching impulses, the type of breakdown largely dependant on the gap spacing. Breakdown can occur in one gap (between the high voltage electrode and the floating object) and then in the other or simultaneously in both.

For streamer breakdown in the first gap, the applied voltage, U_1, needed is :

$$U_1 = u_g + E_{cr} d_1 \qquad \text{(A.29)}$$

where u_g = the approximate floating object potential

E_{cr} = the critical streamer gradient = 400kV/m for a rod-plane configuration

d_1 = the primary gap length (between the high voltage electrode and the object)

For streamer breakdown in the second gap, the voltage required on the floating object, U_{s2} is :

$$U_{s2} = E_{s2} \cdot d_2 \qquad \text{(A.30)}$$

where E_{s2} = the critical streamer gradient = 400kV/m for a rod-plane configuration

d_2 = the secondary gap length (between the floating object and ground)

The overall voltage on the floating object, u_f, is in general more than just u_g, and is given by :

$$u_f = u_g + u_c + u_i \qquad \text{(A.31)}$$

where u_g = the geometric potential

u_c = the potential due to accumulated free charge which in the case of a protrusion on the floating object, is reduced.

u_i = the potential induced due to space charge in the gap. This and the geometric potential can be calculated by a charge simulation technique.

If the voltage on the floating object is insufficient to break down the secondary gap, the result of breakdown in the primary gap will increase the potential on the floating object to U_{fs}, given by :

$$U_{fs} = U_1 - U_R \qquad \text{(A.32)}$$

where U_R = the voltage drop of a leader of length d_1

For leader breakdown of the gaps, the leader inception voltage is in general given by *equation A.21*.

Rizk has produced an empirical formula to determine the minimum value of the 50% breakdown voltage, U_c, for a rod-plane gap configuration with a floating object, which is related to the breakdown voltage for the same configuration without a floating object, U_o

.

$$\frac{U_c}{U_o} = 1 - (\frac{l_o}{d})^{0.4} \qquad \text{(A.33)}$$

where d = the overall gap length from the high voltage electrode to the ground plane

l_o = the diameter of the floating object plus the length of its protrusion

The formula is only valid for $3 \leq d \geq 12$ m and $l_o/d \leq 0.45$.

Article 33 :

-Rizk analysed streamer and/or leader inception and hence breakdown for phase to ground and phase to phase configurations with floating objects under switching impulses.

The phase to ground formulations are the same as in article 3 although specific equations, following *equation A.21* are given for the leader inception voltage in the rod-plane gap and conductor plane configurations.

The phase to phase formulations for the leader inception voltage is given by *equation A.26*

The breakdown voltage is then calculated from the best combination of the most feasible situations in the primary and secondary gaps leading to the minimum total breakdown voltage.

The empirical formula listed as *equation A.33* for the rod-plane gap is presented. The gap factors are given for the conductor-plane (1.15) and the tension string (1.05).

In phase to phase configurations, an empirical formula is presented which is valid for interphase distances of 8 and 12m and floating objects of total length (including

protrusion) in the range 1.1 to 4.4m for α=0.5 and 0.33, where α is the relation between the positive impulse on one phase and the negative impulse on the other phase, defined as follows :

$$\alpha = \frac{U_a}{U_a + U_b} \tag{A.34}$$

The empirical formula for the minimum value of the 50% breakdown voltage with a floating object, U_c, relative to the 50% breakdown voltage without a floating object, U_o, in phase to phase systems, under the above-mentioned constraints is :

$$\frac{U_c}{U_o} = 0.59 - 0.65(\frac{l_o}{d}) \tag{A.35}$$

or to within 6% accuracy can be estimated using :

$$\frac{U_c}{U_o} = \sqrt{1 - \sqrt{\frac{l_o}{d}}} \tag{A.36}$$

where l_o = the total length, including protrusion, of the floating object

d = the overall gap length between the phase conductors

Working Group 33.07 and Task Force 33.07.09

Article 8 :

-This paper shows that the strength of a gap during live working can be expressed by :

$$U50 = K.Cd.Cw.Ca.U_{50p} \tag{A.37}$$

where K is the gap factor = 1 (rod-plane), 1.2.1.1 (phase-structure), 1.6/1.45 (phase-phase)

Cd = a correction for the damaged insulator string

$= 1-0.8Bn_d/n_s$

where B = 1 (broken toughened glass insulators), 0.75 (punctured porcelain insulators)

n_d = the number of damaged units

n_s = the total number of units in the string

Cw = correction for extraneous objects in the gap such as tools or the worker

= 0.9 and 0.85 for phase to ground and phase to phase respectively where the object is in contact with the high voltage electrode and thus a gap factor of 1.2 and 1.6 for phase to ground and phase to phase need to be used as the conductor structure has been modified to a rod-structure.

= 1 when the object is at ground potential and the gap factor remains unchanged or increases.

= 0.85 and 0.8 for phase to ground and phase to phase respectively where the object is at floating potential and gap factors of 1.2 and 1.6 for phase to ground and phase to phase configurations exist. The floating object in this case has a length higher than 0.05 that of the air gap. A graph relating Cw to the gap factor used for floating objects is provided in the article.

Ca = a correction for atmospheric conditions

$= 0.8[1+T(1-\delta)](\delta-0.2g)/(1-0.2g)+0.2$

where $T = 1.4K^{1.4}[1-0.8g^3(1-0.2g)]$

$g = U_{50}/\{500D[1+(K-1)/3]\}$

where U_{50} is the U_{50} under standard conditions and D is the gap length

$\delta = e^{-\alpha A}(273+to)/(273+t)$

where A = altitude in metres, $\alpha = 121.10^{-6}$, to = 20°C and t is in °C

$U_{50} = 1080 \ln(0.46D+1)$ which is in kV and valid for gap spacing in the range 0.5 to 12m

In phase to phase systems the dielectric strength of the air is given by :

$$|U^+| + |U^-| = KU_{50rp} \tag{A.38}$$

where U^+ and U^- = the potential on each phase.

The gap factors shown earlier for phase to phase configurations are valid for α=0.5 where α is defined as in *equation A.34*.

Kishizima, Matsumoto, Watanabe

Article 13 :

- Shows that the critical time to crest in microseconds is given by 55d where d is the gap spacing in metres.
- Summarises the U_{50} formulas that are available for rod-plane gaps :

$U_{50} = 3450/(1+8/d)$ (Dr. G. Gallet et.al)

$U_{50} = 1350d^{0.43}/(1.31+2.11/d)$

$U_{50} = 1080 \ln(0.46d+1)$

All these are said to be accurate to within 3% in the range of *d* from 2 to 12m.

- The paper also states that the switching impulse phase-phase flashover voltage depends on the gap spacing, a variable α defined in equation 34 and the time to crest.

Carrara and Thione

Article 14 :

- The various stages in the breakdown process are briefly described from corona inception with the dark periods that follow as a result of space charge produced, to leader inception and its dark periods, continuous leader inception, the final jump and breakdown. Breakdown follows at the point of the final jump which only occurs when pre-leader streamers from the continuous leader stage bridge the gap. Hence, much work

has been done to understand the breakdown process in long gaps based on the final two stages and the transition from continuous leader to the final jump. The change in voltage from the continuous leader inception voltage to the final jump voltage is very slight and occurs at the crest of the applied voltage waveform which has a gradual slope compared to the slope between corona inception and the continuous leader inception.

- The concept of a critical radius of the electrode is introduced, below which the sparkover voltage remains constant and no longer decreases. Above this radius, the sparkover voltage will increase. Above a critical radius, the primary dark periods do not exist whereas they do below the critical radius and hence above a critical radius, the corona inception voltage is assumed as coinciding with the leader inception voltage.

- The paper presents an approach whereby the breakdown voltage is made up of three components :

$$U_{50} = U_i + \Delta U_l + \Delta U_\sigma \qquad (A.39)$$

where U_i = the continuous leader inception voltage

ΔU_l = the leader propagation voltage increase

ΔU_σ = the statistical voltage increase between the U_{50} and the U_B

U_i is determined from the critical electrode radius (which has been evaluated in this paper for rod-plane and conductor-plane gaps and varies with gap separation) and the critical corona inception field which is experimentally determined. A method is given for calculating the critical electrode size for a variety of other configurations. By using a field calculation program with the known critical radius and corona inception field, the continuous inception voltage can then be calculated as the corresponding corona inception voltage. Alternatively, Maxwell 3D enables the electric field to be evaluated for any geometry and thus the critical field can be determined by using the work of either Zaeng , Heymann or Peek as discussed above. The justification behind equating the corona inception voltage with the continuous leader inception voltage seems to be as a result of the concept of a critical electrode size.

ΔU_l is evaluated as follows. The leader length, l, prior to the final jump is calculated as follows :

$$l = d - U_l / E_s \qquad \text{(A.40)}$$

where d = gap length

E_s = average streamer gradient = 4kV/cm

The leader propagation time, ΔT_l, is then = l/v where v is the velocity of the leader = 1.5cm/μs. ΔU_l is then evaluated from a table relating the leader propagation time and effective gap length to the leader voltage rise.

The U_{50} is then given as :

$$U_{50} = \frac{U_l + \Delta U_l}{1 - \gamma\sigma} \qquad \text{(A.41)}$$

where γ = a factor for the sparkover probability = 3

σ = the standard deviation of the sparkover probability function = 0.05

Kosztaluk, Lanoie, Malewski, Menemenlis, Nguyen

Article 18 :

- This deals with phase-phase flashovers influenced by the time difference between the crests of the positive and negative impulses on each conductor. The phase-phase flashover voltage, U_{pp}, for a time difference, $\Delta T_{cr} = 0$, is best expressed by the empirically determined regression curve :

$$U_{pp} = \frac{U_{ss}}{\left[1 - \alpha\left(1 - \frac{U_{ss}}{U_0}\right)\right]} \qquad \text{(A.42)}$$

where V_{50}^{+} and V_{50}^{-} are the values of V^{+} and V^{-} corresponding to the 50% breakdown probabilities for $V^{-} = 0$ and $V^{+} = 0$ respectively (V^{+} and V^{-} are the conductor voltages on each of the two phases considered).

- The phase-phase breakdown voltage for ΔT_{12} exceeding 1 to 2 ms where the negative impulse precedes the positive impulse, is considerably lower than for $\Delta T_{12} = 0$. This is explained by the formation of space charge when the first impulse occurs which changes the field strength. This drop in breakdown voltage increases as V^{+} increases. This drop also increases as ΔT_{12} increases until a certain maximum ΔT_{12} after which it again increases to the value corresponding to $\Delta T_{12} = 0$.

Gallet, Leroy, Lacey, Kromer

Article 22 :

- The paper criticises the expression produced by Paris as being suitable for the E.H.V. range with 2 to 8m gap lengths, but not suitable for the U.H.V. range :

$$U_{50} = k.500.d^{0.6} \qquad (A.43)$$

where k = gap factor
d = gap length

- The paper produces and empirical formula for the breakdown voltage for any gap geometry valid in a range from 1 to 30m and subject to positive switching impulses :

$$U = k\frac{34}{1+\frac{8}{d}} \quad (MV,m) \qquad (A.44)$$

- It is also suggested that the gap factor ought to be modified based on statistics due to parallel discharge paths.

Hutzler, Garbagnati, Lemke, Pigini

Article 26 :

- Presents formulas for U_{50} as follows :

$$U = \frac{3400}{1+\frac{8}{d}}$$ for gap lengths of 2-15m and where the anode radius < critical radius

$$U = 1400+55d$$ for gap lengths from 15-30m (A.45)

$U = 1080 \ln(0.46d+1)$ for larger gaps up to 25m

$U = 500.d^{0.6}$ for 250/2500μs impulses up to 10m

$U = 1180d^{0.45}$ for negative impulses with gap lengths from 2-14m

- The paper makes the statement that for a pointed cathode there is a higher flashover voltage than for a pointed anode. It also introduces very detailed formulas for the gap factor in various geometry's, how it is modified for bundles, the relation between the critical time to crest and the gap factor. The modification of the gap factor is shown for insulators, post-insulators such as floating objects and for rain. It is then shown how the gap factor is used in the calculation of the phase-ground and the phase-phase breakdown voltages.

Schaeider, Week

Article 30 :

- This paper states that the breakdown voltage for a 2-8 m gap and ideal for a 120μs impulse can be expressed by *equation A.43*, while where the time to crest varies according to the gap distance and ideal for long gaps the breakdown voltage can best be expressed by *equation A.44* with the numerator (3.4) replaced with 3450 and the voltage expressed as kV.

- The paper only deals with positive switching impulses. The gap factor for a specific geometry is expressed as the ratio of the U_{50} for that geometry to the U_{50} for a rod-plane gap. The gap factor is a function of the inhomogeneity of the field, determined by the shape of the positive electrode, as well as of the symmetry of the field distribution which for a given positive electrode is determined by the shape of the grounded electrode. Thus from any E-field distribution, we are able to calculate the gap factor and hence by using available formula, the breakdown voltage can be determined. This modelling technique is not suitable for gaps < 3m and for fields with low divergency.

The inhomogeneity, F_i, of the field, E, is evaluated as :

$$F_i = \int_0^{x_i} E(x)dx \qquad \text{(A.46)}$$

whilst the symmetry, F_s, of the field is evaluated as :

$$F_s = \int_0^{x_s} E(x)dx \qquad \text{(A.47)}$$

where x_i is the distance from the ground electrode to the point where the E-field is equal to the field strength of the homogeneous gap, which is approximated at $0.9d$ and where x_s is the distance from the ground electrode to the point where the E-field is minimum, which is approximated at $0.4d$. The paper presents a graph relating the gap factor to the ratio of F_s to F_i.

Baldo, Hutzler, Pigini, Rizk

Article 31 :

- The paper presents an accurate description of the physics involved with the first corona, the leader phase, the final jump and the influence of the impulse shape. A number of models for switching impulse breakdown are listed :

Lemke :

The breakdown voltage is the sum of the leader voltage drop and the streamer voltage drop which precedes the leader. The expression is given as :

$$U_{50} = aE_s\left[1 + \ln\left(\frac{d}{a}\right)\right] + aE_{la}\ln\left[\frac{d}{a} - \ln\left(\frac{d}{a}\right)\right] \qquad \text{(A.48)}$$

where E_s = the mean streamer gradient = 4.5kV/cm

d = gap length

E_{la} = a constant taken as 1.5kV/cm

a = an unknown constant which varies with electrode configuration. To fit experimental results a = 1m for rod-plane and 1.5m for bundle conductor-plane, 1.3m for bundle conductor-tower.

Aleksandrov :

A critical charge at the high voltage electrode, q, which is a combination of the electrode charge at the corona onset voltage as well as the space charge at leader inception, is a prerequisite for continuous leader development. The charge does not depend on the gap length. If the conductor-plane breakdown voltage can be determined for two different gap spaces by experimental or other means, say, U_1 and U_2, then the breakdown voltage for a third configuration, U_3, can be determined as follows :

$$U_2 - U_1 = \Delta U_{12} = \frac{q}{2\pi\varepsilon_0}\ln\left(\frac{d_2}{d_1}\right) \qquad \text{(A.49)}$$

$$U_3 - U_1 = \Delta U_{13} = \frac{q}{2\pi\varepsilon_0}\ln\left(\frac{d_3}{d_1}\right) \qquad \text{(A.50)}$$

and thus using *equation A.49* : $$\Delta U_{13} = \Delta U_{12}\frac{\ln\left(\frac{d_3}{d_1}\right)}{\ln\left(\frac{d_2}{d_1}\right)} \qquad \text{(A.51)}$$

Further models and analytical expressions are suggested by Jones, Hutzler and Bazelyan. Boutlendj, Allen, Sparrow

Article 35 :

- This paper presents an equation for the breakdown voltage across insulator strings :

$$U_b = U_0\left(1 - 0.8\frac{n_b}{n_0}k\right) \tag{A.52}$$

where U_b = the breakdown voltage with n_b broken units

U_0 = the breakdown voltage with n_0 healthy units

k = coefficient representing the average state of the broken unit. It varies between 0 and 1.

When arcing horns are taken into account, *equation A.52* can be modified by replacing the factor 0.8 and the coefficient k with 1.

Task Force 07.02 of Study Committee 33

Article 38 :

- Describes the influencing factors which affect the dielectric strength of air gaps containing floating objects.

- For a rod-plane gap where the object is connected to the high voltage electrode, the strength is :

$$U_{50} = \frac{3400}{1 + \dfrac{8}{D - d_1 - L}} \tag{A.53}$$

and when it is connected to the ground it is :

$$U_{50} = \left(1 + 0.6\frac{D - d_1}{D}\right)\frac{3400}{1 + \frac{8}{d_1}} \qquad \text{(A.54)}$$

where D = gap length

L = length of object along gap axis

d_1 = primary gap length.

The breakdown voltage for the primary and secondary gaps, U_1 and U_2 respectively can be determined by the gap capacitance's as follows :

$$U_1 = \left(1 + \frac{C_2}{C_1}\right)U_{1b} \qquad \text{(A.55)}$$

$$U_2 = \left(1 + \frac{C_1}{C_2}\right)U_{2b} \qquad \text{(A.56)}$$

where C_1 and C_2 = the capacitance of the primary and secondary gaps respectively

U_{1b} and U_{2b} = the breakdown voltages of the primary and secondary gaps respectively independent of the other gap

- The critical conditions are summarised as follows .
  - for positive overvoltages
  - for objects with anodic protrusions
  - for objects lying on or near the gap axis at a critical distance d_{1c} from the energised electrode
  - for objects with a large cross section
  - for long objects

For a large range of parameters it has been shown that the critical conditions are .

$$0.2 < \frac{d_w}{D} < 0.39 \quad \text{and} \quad U_s = U_0(0.6 + 0.02D - 0.54\frac{l}{D}) \qquad \text{(A.57)}$$

where U_0 = the breakdown voltage without a work object

- The breakdown voltage across insulator strings is given by *equation A.52* where k is said to have an average value of 0.75 although it is most conservative to have a value of 1.

Taudiere, Lalot

Article 39 :

- The paper deals with phase to phase flashovers with floating objects. A formula is derived from which the minimum spacing between the floating object and the phase conductors can be determined in order to prevent flashover :

$$\frac{1+\frac{8}{T_i}}{1+\frac{8}{T}} = 0.85 \qquad \text{(A.58)}$$

where T_i = the sum of the primary and secondary gaps

T = the gap distance without a floating object

Hutzler

Article 41 :

- In this paper Hutzler shows that with a smooth floating object the breakdown voltage is higher. This is because positive charge from the electrode is deposited and builds up radially around the floating object. As a result the discharge would move around the floating object and therefore the voltage and time to breakdown is higher than without the breakdown object. If the object has a protrusion, the breakdown voltage is lower because the discharge occurs from the object.

- Hutzler presents *equations A.53* and *A.54* which represents a rod-plane gap (when breakdown has occurred in the primary gap and hence the floating object is connected to the electrode) and a rod-rod gap (when breakdown has occurred in the secondary gap and hence the floating object is connected to ground). By equating these two equations, the critical primary gap length and gap strength is determined which is shown in *equation A.57*.

- The longer the protrusion length and the greater the protrusion diameter, the lower the breakdown strength.

Lloyd, Zaffanella

Article 42 :

- A correction for humidity and air density is shown. Either the voltage is corrected or the gap spacing is corrected. The voltage correction is :

$$U_{std} = U_{test}\left(\frac{H_u}{\delta}\right)^n \qquad \text{(A.59)}$$

The gap spacing correction is : *

$$S_{std} = S_{test} H_s \delta \qquad \text{(A.60)}$$

where U_{std} and S_{std} = the voltage and gap spacing under standard conditions respectively

U_{test} and S_{test} = the voltage and gap spacing under test conditions respectively

δ = the relative air density given by *equation A.1*

H_u and H_s = humidity voltage and spacing correction factors given by graphs in the article.

n = a factor which may vary for H_u and δ also given by a graph in the article.

Alternatively, a correction factor, K^n, can be applied where :

$$K = 0.997\text{-}0.106A$$

where A = altitude in km

and $n = 1$ for $d \leq 1$

$= 1.12 - 0.12d$ for $1 < d < 6$

$= 0.4$ for $d > 6$

where d = gap length in meters

During rain, the positive U_{50} for switching impulses is typically 0.95 the dry value and for negative impulses rain can reduce the strength to that of the positive strength. The insulator string length must be $1.05d$ - $1.1d$ otherwise the breakdown voltage can drop by up to 20% during rain, fog and high humidity conditions.

- The relation between critical time to crest, T_c , and gap spacing, S, is given by :

$$T_c = 545 - 60 \qquad \text{(A.61)}$$

For a time to crest which is not critical as determined by *equation A.61*, either the voltage needs to be corrected or the gap spacing needs to be corrected such that the time to crest is then critical. This is done by calculating the difference between the time to crest applied and the critical time to crest as calculated by *equation A.61* and then using a table or figure provided in the article to obtain the correction.

- The work also summarises that of Carrara and Thione's model :

1. Decide whether gap is of the rod (spheres, rods, and line terminations) or conductor (conductor-ground, conductor-objects, conductor-tower, station buses) configuration.
2. Using a 3D field plotting program, calculate the ratio of V to E at a distance r from the electrode, arbitrarily selected as 40cm for rods and 15cm for conductors.

3. If the configuration is not rod-plane or conductor-plane, then calculate an effective gap distance, D_e, from the following equations :

$$\left(\frac{V}{E}\right)_{r=40cm} = \frac{\frac{1}{40} - \frac{1}{2D_e - 40}}{\frac{1}{40^2} + \frac{1}{(2D-40)^2}} \text{ cm} \quad \text{(rod-plane)} \qquad \text{(A.62)}$$

$$\left(\frac{V}{E}\right)_{r=15cm} = \frac{15(2D_e - 15)}{2D_e} \ln\frac{2D_e - 15}{15} \text{ cm} \quad \text{(conductor-plane)} \qquad \text{(A.63)}$$

4. Calculate the critical radius using the gap distance (or effective gap distance) :

$$R_c = 38(1\text{-}D^{D\,500}) \text{ cm} \quad \text{(rod-plane)} \qquad \text{(A.64)}$$

$$R_c = 3.7\ln(1+D/100) \text{ cm} \quad \text{(conductor-plane)} \qquad \text{(A.65)}$$

5. Calculate the ratio K between the voltage and field at the electrode surface using the critical radius or the actual radius should that be greater than the critical.
6. Determine the leader inception voltage $V_i = KE_c$, where E_c is a function of the critical radius giving the critical field at which corona starts.
7. Calculate the leader length, $l = D - S$ where $S = V_i / E_s$ for E_s between 4 and 5.5 kV/cm.
8. Using a graph in the article, the leader voltage drop, ΔV, is found from the leader length.
9. The critical flashover voltage is then found, $U_{50} = V_i + \Delta V + 0.15\ U_{50}$.

Refinements have been made to this model some of which make it adaptable for evaluating multielectrodes, phase-phase and waveshapes other than critical.

List of articles

Article 2 - "High Voltage Engineering Fundamentals", E. Kuffel, W.S. Zaengl, Pergamon Press, 1984

Article 3 - "Effect of conducting objects on critical switching impulse breakdown of long air gaps", F.A.M. Rizk, CIGRE, 1994, 28 August-3 September

Article 8 - "Dielectric strength of external insulation systems under live working", Working Group 33.07 and Task Force 33.07.09, CIGRE, 1994, 28 August - 3 September

Article 9 - "Switching impulse strength of air insulation : leader inception criterion", F.A.M. Rizk, IEEE Transactions on Power Delivery, Vol. 4, No. 4, October 1989

Article 11 - "Corona on conductor bundles", F.G. Heymann, SAIEE Transactions, Volume 57, November 1966, Part 11

Article 12 - "Corona on wires in air", F.G.Heymann, SAIEE Transactions, Volume 56, November 1965, Part 11

Article 13 - "New facilities for phase-phase switching impulse tests and some test results", I. Kishizima, K. Matsumoto, Y. Watanabe, IEEE Transactions on Power Apparatus and Systems, Vol. PAS-103, No.6, June 1984

Article 14 - "Switching surge strength of large air gaps", G. Carrara, L. Thione, IEEE Transactions on Power Apparatus and Systems, Vol. PAS-95, No.2 , March/April 1976 .

Article 18 - "Effect of the time shift between the two voltage components on phase-phase insulation strength", R. Kosztaluk, R. Lanoie, R. Malewski, C. Menemenlis, D.H. Nguyen, IEEE Transactions, IEEE Transactions on Power Apparatus and Systems, Vol. PAS-100, No. 7, July 1981

Article 20 - "A model for switching impulse leader inception and breakdown of long air gaps", F.A.M. Rizk, IEEE Transactions on Power Delivery, Vol. 4, No. 1, January 1989

Article 22 - "General expression for positive switching impulse strength valid up to extra long air gaps", G. Gallet, G. Leroy, R. Lacey, I. Kromer, IEEE Transactions on Power Apparatus and Systems, Vol. PAS-94, No.6, November December 1975

Article 26 - "Strength under switching overvoltages in reference ambient conditions", B. Hutzler, E. Garbagnati, E. Lemke, A. Pigini

Article 30 - "Parameters influencing the gap factor", K.H. Schneider, K.H. Weck

Article 31 - "Fundamentals of the discharge mechanisms and description of the phenomena by physical-mathematical models", G. Baldo, B. Hutzler, A. Pigini, F. Rizk

Article 32 - "Critical switching impulse strength of phase-phase air insulation", F.A.M. Rizk, IEEE Transactions on Power Delivery, Vol. 8, No. 3, July 1993

Article 33 - "Effect of floating conducting objects on critical switching impulse breakdown of air insulation", F.A.M Rizk, IEEE Transactions on Power

Delivery, Vol. 10, No. 3, July 1995

Article 35 - "Impulse performance of insulator strings with defective units for 132kV and 400kV towers", M. Boutlendj, N.L. Allen, L.J. Sparrow, 9th ISH, August 28 -

1 September 1995

Article 38 - "Strength of external insulation during live line maintenance and repair work with special reference to transient overvoltages", Task Force 07.02 of Study Committee 33

Article 39 - "Dielectric strength of phase-phase air clearances including a metallic body at floating potential", I. Taudiere, J. Lalot, 7th ISH, August 26-30, 1991

Article 41 - "Switching impulse of air gaps containing a metallic body at floating potential", B. Hutzler, 5th ISH, 24-28 August, 1987

Article 42 - "Insulation for switching surges", K.J. Lloyd, L.E. Zaffanella, (EPRI Transmission Line

Appendix B

B.1 Formulation for the Continuous Leader Inception Criterion

From Rizk's paper [Rizk Oct. 1989], a criterion for the continuous leader inception voltage has been used to determine the continuous leader inception voltage for the rod-plane, conductor-plane and tower-conductor window geometry's. This formulation of this criterion is now presented in detail.

When the insulating strength of air is exceeded, streamers develop from the high voltage electrode and sufficient ionisation may lead to an ionised zone. Stress on the surrounding air as a result of this ionised zone will lead to several streamers developing from the tip of the zone. Thus each zone will have a multitude of streamers which are convergent at the tip of the ionised zone. This is depicted in *Figure B.1*. In order for a positive leader to grow as an sustained extension of this ionised zone, the difference between the applied field, E_a, and the opposing space charge field, E_{sc}, must equal or exceed a certain critical field strength, E_c. This relation is shown below in *equation B.1* :

$$E_a - E_{sc} \geq E_c \tag{B.1}$$

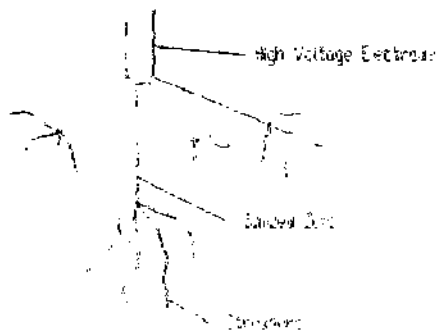

Figure B.1 - Continuous Leader Inception

The field strengths can be converted to voltages by using the equation that relates the electric field of a point charge to the voltage on the charge, shown in *equation B.2*.

$$E = \frac{V}{r} \tag{B.2}$$

All voltages concerned are with reference to a plane which can be regarded as lying in the far field for large air gaps. Hence, the applied E-field at the tip of the ionised zone, can, in the far field, be equated to that of a point charge. The space charge can effectively be modelled as a singular point charge ahead of the ionised zone. If the voltage is measured at a distance r from the tip of the ionised zone, where r is much smaller than the distance from the ionised zone tip to an equivalent centre of the space charge and independent of the gap spacing, then the following relations apply :

$$\begin{aligned} E_{ic} &= \frac{U_{ic}}{r} \\ E_{sc} &= \frac{\alpha U_{sc}}{r} \\ E_{c} &= \frac{U_{c}}{r} \end{aligned} \tag{B.3}$$

where U_{ic}, U_{sc} and U_c are the continuous leader inception, space charge and critical voltages respectively. The constant α is a proportionality constant which is a function of the ratio between r and the distance between the tip of the ionised zone and the equivalent centre of the space charge.

From *equations B.1* and *B.3*, the minimum value for the continuous leader inception voltage is :

$$U_{ic} - \alpha U_{sc} = U_c \tag{B.4}$$

The space charge voltage is made up of two components. The first component, U_{sa}, is the induced voltage due the effective critical space charge, Q_o. The second component U_{sb} is the absolute value of the induced voltage as a result of image charges induced on the opposite electrode and other nearby objects, due to the space charge Q_o and any charge that it induces on the high voltage electrode. If the effective centre of the total space charge Q_o is at a distance s from the high voltage electrode and the induced voltage due to the various components of the space charge is measured at a point P situated at a distance s_o from the high voltage electrode, then the magnitude of the two components of the space charge is represented as follows :

$$U_{sa} = \frac{Q_o}{4\pi\varepsilon_o(s - s_o)} \tag{B.5}$$

$$U_{sb} = \frac{Q_o}{4\pi\varepsilon_o R} \tag{B.6}$$

The induced voltage due to image charges is made up of an unknown R which is a function of the gap spacing and electrode configuration and which can be determined analytically but more appropriately by a charge simulation technique. The total space charge voltage, U_{ss}, is then the difference between U_{sa} and U_{sb} as shown in *equation B.7*.

$$U_{ss} = U_{sa} - U_{sb} \tag{B.7}$$

Substituting for U_{sa} and U_{sb} from *equation B.5* and *equation B.6* respectively, *equation B.7* can be represented as follows :

$$U_{ss} = \frac{Q_o}{4\pi\varepsilon_o(s - s_o)} - \frac{Q_o}{4\pi\varepsilon_o R} \tag{B.8}$$

Substituting for U_{ss}, *equation B.4* becomes :

$$U_{hv} = \frac{\alpha Q_o}{4\pi\varepsilon_o(s - s_o)} + \frac{\alpha Q_o}{4\pi\varepsilon_o R} = U_s \tag{B.9}$$

At the transition from streamer corona to leader inception, the injected charge, Q_s will reach a critical value and is assumed to be proportional to the continuous leader inception voltage for a specific high voltage geometry. Hence, the quotient, c of Q_s and U_{ic} will also assume a critical value. This value varies with the electrode geometry as the critical charge varies depending on the type of electrode geometry. However, c is independent of the gap spacing. Substituting for c into *equation B.9* and making U_i the subject of the formula, the continuous leader inception voltage is formulated and is shown in *equation B.10*.

$$U_{ic} = \frac{U_{ic\infty}}{1+\frac{A}{R}} \tag{B.10}$$

where $U_{ic\infty} = \dfrac{U_c}{\left[1-\dfrac{\alpha c}{4\pi\varepsilon_0(s-s_{cr})}\right]}$ and $A = \dfrac{\dfrac{\alpha c}{4\pi\varepsilon_0}}{\left[1-\dfrac{\alpha c}{4\pi\varepsilon_0(s-s_{cr})}\right]}$

The format of *equation B.10* is very well known [Gallet, Leroy, Lacroix & Fromer] and has been empirically derived before. The formula produced by Rizk for the continuous leader inception voltage can be applied to any rod-type and conductor-type geometry. The values of $U_{ic\infty}$ and A have been determined empirically [Rizk Jan. 1989]. For the rod-type gaps $U_{ic\infty}$ and A assume the values of 1556kV and 7.78m respectively. For the conductor-type gaps $U_{ic\infty}$ has the value of 2247kV and A is dependant on how the geometric model is defined. This dependence of A in conductor-type gaps is elaborated on in *Chapter 4*. *Equation B.9* can thus be used to determine the continuous leader inception voltage for any rod-type and conductor-type geometry. The only unknown which needs to be determined is R which takes into account the influence of image charges. The value of R can be expected to vary significantly for rod-type and conductor-type geometry's as the surface area on which the critical charge Q_s is induced varies for the different geometrical configurations.

B.2 The Charge Simulation Technique

In order to evaluate the value of R in *equation B.6* which accounts for the influence of the image charges in the total induced voltage as a result of space charges, the user either has adopt an analytical approach or make use of a charge simulation technique. An analytical approach is rather straightforward for simple geometry's such as the rod-plane gap but becomes far more impractical to use for more complex geometry's. Thus, in determining the magnitude of R for the tower-conductor window geometry where a number of ground planes exist depending on the shape of the window, a charge simulation technique has been used. Charge simulation has been used for the rod-plane and conductor-plane gaps in order to gain confidence with the simulation where simulation results can be compared to those that would be obtained where analytical derivations are still easy to obtain, particularly for the rod-plane gap. Since unsatisfactory results were obtained using the *Maxwell 2D* and *3D* finite element packages, the 3D charge simulation package, *Coulomb* was tested which produced satisfactory outputs that corresponded favourably with analytical results. Contrary to *Maxwell* which meshes the air gap around the electrode surfaces and uses the derivative of Maxwell's equations to calculate potentials in the air gap, *Coulomb* only meshes the electrode surfaces and integrates Maxwell's equations. Thus in order to obtain a high level of accuracy using *Maxwell*, a large mesh is required in the air-gap whereas for *Coulomb* a sufficiently meshed electrode surface will allow a satisfactory level of accuracy to be achieved as a result of a number of electrostatic charges from the electrode having their potentials superimposed at the point of measurement in the air gap. Results from *Coulomb* for a point charge in space were compared with that of *Maxwell* and were found to be far more accurate than that of *Maxwell* when compared with theory. This confirmed the suspicions that arose regarding the accuracy of using *Maxwell*. Furthermore, the new version of *Maxwell 3D* has a bug whereby specifying a charge is not a sufficient source of excitation. This problem does not exist in the old version of *Maxwell 3D*. However, simulations on the old version are too slow whereas *Coulomb* is faster in comparison and thus more convenient.

The procedure for using a charge simulation technique is as follows. The geometry being studied is entered into a charge simulation program. Experience with *Coulomb* has found

that it is necessary to specify the image of the high voltage electrode and hence exclude the ground plane rather then including a ground plane and expecting the image to be calculated automatically. A point charge, Q_p, is placed at P in the z-plane between the high voltage electrode and imaginary ground plane at a distance s from the high voltage electrode. The image of this point charge also needs to be entered into the simulation program, with the overall effect of having the high voltage electrode and the point charge as well as their respective images being specified in the simulation program.

The simulation is then run and once a solution is obtained, the accuracy of which depends on the number of segments specified in the case of *Coulomb* or the number of triangles in the case of *Maxwell*, the magnitude of the voltage is measured at a point s_2 between the point charge and the high voltage electrode. This voltage, U_m, represents the total voltage induced by the space charge which is made up of two components. The first is the directly induced voltage by the point charge and the second component is the induced voltage due to image charges of the point charge on the high voltage electrode, other nearby objects and the opposite electrode, the latter often just being the ground electrode.

The measured voltage, U_m, is subtracted from the direct influence term, U_{ip}, shown in *equation B.5* to give the induced potential due to the image charges of the point charge, U_{ip}, given by *equation B.6*. Since the arbitrarily chosen charge, Q_p, is known, the value of R can be determined.

The above description of the charge simulation technique is shown graphically in *Figure B.2* below for a conductor-plane gap in 2D. The conductor radius is denoted by a and the gap length by d.

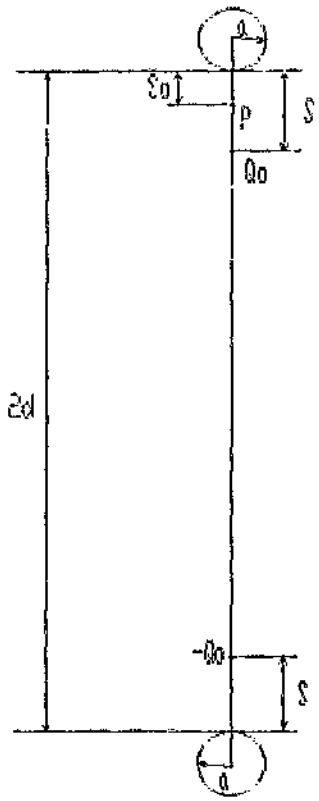

Figure B.2 - The Charge Simulation Technique

B.3 The Leader Voltage Drop

In addition to the continuous leader inception voltage, the second component which makes up the breakdown voltage is the leader voltage drop. Rizk has derived an expression for the leader voltage drop which can be used to determine the voltage drop in leaders for both rod-type and conductor-type gaps [Rizk Jan. 1989].

The leader conductance per unit length, G, is assumed [Jones], based on its resemblance to an arc, to be represented by a dynamic equation [Hochrainer] shown in *equation B.11* for constant current leader propagation.

$$G(t) = G_o + (G_i - G_o)\exp(\frac{-t}{\theta}) \tag{B.11}$$

G_i and G_o are the initial and final values of the leader conductance respectively, t is the life time of the leader section and θ is a time constant in the range 30-60μs. Under critical conditions, the leader propagates with a velocity v = 1.5cm/μs and thus the conductance can be expressed as :

$$G(t) = G_o + (G_i - G_o)\exp(\frac{-x}{x_o}) \tag{B.12}$$

where x is the displacement in time t and x_o is constant at 0.75m assuming a value of θ= 50μs. Ohm's law relates the leader conductance, G, to the leader gradient, E_l, and the leader current, i_l, in *equation B.13*. The leader gradient can then be used to obtain the leader voltage drop, ΔU_l, for any leader length, l_l, as shown in *equation B.14*.

$$E_l = \frac{i_l}{G} \tag{B.13}$$

$$\Delta U_l = \int_0^{l_l} E_l(x)\,dx \tag{B.14}$$

Substituting for G and integrating *equation B.14* :

$$\Delta U_l = l_l E_o + x_o E_i \ln[\frac{E_i}{E_o} - \frac{E_i - E_o}{E_o}\exp(\frac{-l_l}{x_o})] \tag{B.15}$$

where E_i and E_o are the initial and final values of the leader gradient which assume values of 400kV/m and 50kV/m respectively [Jones]. Substituting values for x_o, E_i and E_o into *equation B.15*, the following expression is obtained for the leader voltage drop in rod-type or conductor-type gaps :

$$\Delta U_1 = 50 l_2 + 37.5 \ln[8 - 7\exp(-1.33 l_2)] \tag{B.16}$$

B.3.1 The Rod-Type Gap

The leader length at the point of the final jump prior to breakdown is obtained by subtracting the height of the final jump, h_f, from the total gap length, d. An expression for the height of the final jump has been obtained empirically by Rizk for the rod-plane gap and is shown in *equation B.17*. It is assumed that this expression can be used to represent the height of the final jump for any rod-type gap.

$$h_f = \frac{3.89}{1 + \frac{3.89}{d}} \tag{B.17}$$

The leader length is therefore :

$$l_2 = \frac{d}{1 + \frac{3.89}{d}} \tag{B.18}$$

Substituting *equation B.18* into *equation B.16*, the expression for the leader voltage drop in the rod-type gap is obtained as follows :

$$\Delta U_1 = \frac{50d}{1 + \frac{3.89}{d}} + 37.5 \ln[8 - 7\exp(\frac{-1.33d}{1 + \frac{3.89}{d}})] \tag{B.19}$$

B.3.2 The Conductor-Type Gap

In the conductor-type gap, the height of the final jump is dependant on the gap distance, d, the conductor radius, a, and the leader gradient, E_l. Rizk provides an expression [Rizk Jan. 1989] shown in *equation B.20* from which an approximate value of the leader gradient can be determined.

$$1+\frac{2\frac{k_s}{V_o}(E_g-E_l)}{(\frac{E_{cr}}{V_o}+\frac{1}{d}-\frac{2k_sE_l}{V_o\ln(\frac{2d}{a})})^2 d\ln\frac{2d}{a}}\approx 1.05 \qquad \text{(B.20)}$$

Certain parameters used in *equation 20* are assumed as follows :

- k_s is a shielding factor which is determined empirically and is equal to 0.4
- V_o is a potential related to the charge injected into the leader channel. For a conductor-type gap, charge injection occurs at a rate of approximately 40μC/m which corresponds to a potential of 719kV/m
- E_g is the mean gradient of the pre-leader streamers which for low breakdown probabilities is 400kV/m
- E_{cr} is a gradient which represents the critical field that determines the pre-leader streamer length at the point of final jump when the pre-leader streamers bridge the gap. This gradient has also been empirically determined and is equal to 128kV/m

For a particular value of conductor radius and gap distance, the leader gradient is determined from *equation B.20* and hence the height of the final jump can be evaluated using *equation B.21*. This equation has been empirically determined by Rizk for the conductor-plane gap but it is assumed that it can be used for all conductor-type gaps.

$$h_f=\frac{5.0}{1+\frac{5.0}{d}-\frac{0.5\times10^{-4}E_l}{\ln(\frac{2d}{a})}} \qquad \text{(B.21)}$$

The leader length can then be obtained as the difference between the gap distance and the height of the final jump. The leader voltage drop for conductor-type gaps is then calculated by substituting the value of the leader length into *equation B.16*.

B.4 The Breakdown Voltage

The minimum breakdown voltage, U_m of any rod-type or conductor-type gap is the sum of the continuous leader inception voltage and the leader voltage drop. However, although a theoretical value for the minimum breakdown voltage can be calculated, there is a statistical dependence as to whether breakdown will actually occur. Thus, the breakdown voltage is often quoted as a magnitude at which breakdown has a 50% probability of occurring and is known as the U_{50} value. The 50% breakdown voltage is derived from the minimum breakdown voltage as shown in *equation B.22*.

$$U_{50} = \frac{U_m}{1-3\sigma} \tag{B.22}$$

The standard deviation in the breakdown voltage is given by the parameter σ which assumes a value, usually 5% for rod-type gaps and 3% for conductor-type gaps.

Appendix C

The results for the total induced voltage obtained using the charge simulation technique defined in *Appendix B.2* are listed in this appendix. Tests have been done on the rod-plane, conductor-plane and tower-conductor window geometry's.

Appendix C.1 deals with the change in gap length. Modifications in the model for the rod-plane gap are presented in *Appendix C.2* where the results of changing the value of s, the magnitude of the space charge Q_s and the space charge radius are presented. In *Appendix C.3*, the results of changing the space charge position, adjusting the conductor radius and checking the feasibility of using conductor-bundles in the conductor-plane model, are listed. *Appendix C.4* presents results for additional tests done on the tower-conductor model where the tower window structure is changed and where a tower-conductor-bundle has been examined.

For each specific test, the data has been presented in columns. The first column represents the distance from the high voltage electrode, the second, third and fourth columns are the x, y and z coordinates respectively and the final column is the value of the total induced voltage.

C.1.1 Total Induced Voltage for the 3m Rod-Plane Gap

Distance	X-Coord.	Y-Coord.	Z-Coord.	Value
.0000000	.0000000	.0000000	3000.000	441761.1
2.000000	.0000000	.0000000	2998.000	450929.5
4.000000	.0000000	.0000000	2996.000	460480.0
6.000000	.0000000	.0000000	2994.000	470437.1
8.000000	.0000000	.0000000	2992.000	480827.1
10.00000	.0000000	.0000000	2990.000	491679.1
12.00000	.0000000	.0000000	2988.000	503024.3
14.00000	.0000000	.0000000	2986.000	514897.5
16.00000	.0000000	.0000000	2984.000	527336.2
18.00000	.0000000	.0000000	2982.000	540381.7
20.00000	.0000000	.0000000	2980.000	554079.7
22.00000	.0000000	.0000000	2978.000	568480.2
24.00000	.0000000	.0000000	2976.000	583638.8
26.00000	.0000000	.0000000	2974.000	599616.9
28.00000	.0000000	.0000000	2972.000	616482.8
30.00000	.0000000	.0000000	2970.000	634312.7
32.00000	.0000000	.0000000	2968.000	653191.5
34.00000	.0000000	.0000000	2966.000	673214.6
36.00000	.0000000	.0000000	2964.000	694489.3
38.00000	.0000000	.0000000	2962.000	717136.8
40.00000	.0000000	.0000000	2960.000	741294.3
42.00000	.0000000	.0000000	2958.000	767118.0
44.00000	.0000000	.0000000	2956.000	794786.4
46.00000	.0000000	.0000000	2954.000	824504.5
48.00000	.0000000	.0000000	2952.000	856508.9
50.00000	.0000000	.0000000	2950.000	891073.8
52.00000	.0000000	.0000000	2948.000	928519.3

Distance	X-Coord.	Y-Coord.	Z-Coord.	Value
54.00000	.0000000	.0000000	2946.000	969221.1
56.00000	.0000000	.0000000	2944.000	1013623.
58.00000	.0000000	.0000000	2942.000	1062255.
60.00000	.0000000	.0000000	2940.000	1115749.
62.00000	.0000000	.0000000	2938.000	1174875.
64.00000	.0000000	.0000000	2936.000	1240571.
66.00000	.0000000	.0000000	2934.000	1313996.
68.00000	.0000000	.0000000	2932.000	1396600.
70.00000	.0000000	.0000000	2930.000	1490218.
72.00000	.0000000	.0000000	2928.000	1597210.
74.00000	.0000000	.0000000	2926.000	1720662.
76.00000	.0000000	.0000000	2924.000	1864691.
78.00000	.0000000	.0000000	2922.000	2034907.
80.00000	.0000000	.0000000	2920.000	2239167.
82.00000	.0000000	.0000000	2918.000	2488819.
84.00000	.0000000	.0000000	2916.000	2800884.
86.00000	.0000000	.0000000	2914.000	3202112.
88.00000	.0000000	.0000000	2912.000	3737082.
90.00000	.0000000	.0000000	2910.000	4486043.
92.00000	.0000000	.0000000	2908.000	5609484.
94.00000	.0000000	.0000000	2906.000	7481889
96.00000	.0000000	.0000000	2904.000	0.1122671E+08
98.00000	.0000000	.0000000	2902.000	0.2246156E+08
100.0000	.0000000	.0000000	2900.000	0.4513765E+08

C.1.2 Total Induced Voltage for the 7m Rod-Plane Gap

Distance	X-Coord.	Y-Coord.	Z-Coord.	Value
.0000000	.0000000	.0000000	7000.000	446144.8
2.000000	.0000000	.0000000	6998.000	455315.3
4.000000	.0000000	.0000000	6996.000	464867.9
6.000000	.0000000	.0000000	6994.000	474827.1
8.000000	.0000000	.0000000	6992.000	485219.2
10.00000	.0000000	.0000000	6990.000	496073.3
12.00000	.0000000	.0000000	6988.000	507420.8
14.00000	.0000000	.0000000	6986.000	519296.0
16.00000	.0000000	.0000000	6984.000	531736.8
18.00000	.0000000	.0000000	6982.000	544784.5
20.00000	.0000000	.0000000	6980.000	558484.5
22.00000	.0000000	.0000000	6978.000	572887.2
24.00000	.0000000	.0000000	6976.000	588047.9
26.00000	.0000000	.0000000	6974.000	604028.2
28.00000	.0000000	.0000000	6972.000	620896.2
30.00000	.0000000	.0000000	6970.000	638728.2
32.00000	.0000000	.0000000	6968.000	657609.2
34.00000	.0000000	.0000000	6966.000	677634.4
36.00000	.0000000	.0000000	6964.000	698911.3
38.00000	.0000000	.0000000	6962.000	721561.0
40.00000	.0000000	.0000000	6960.000	745720.6
42.00000	.0000000	.0000000	6958.000	771546.4
44.00000	.0000000	.0000000	6956.000	799217.0
46.00000	.0000000	.0000000	6954.000	828937.3
48.00000	.0000000	.0000000	6952.000	860943.8
50.00000	.0000000	.0000000	6950.000	895510.8
52.00000	.0000000	.0000000	6948.000	932958.5
Distance	**X-Coord.**	**Y-Coord.**	**Z-Coord.**	**Value**

54.00000	.0000000	.0000000	6946.000	973662.5
56.00000	.0000000	.0000000	6944.000	1018067.
58.00000	.0000000	.0000000	6942.000	1066700.
60.00000	.0000000	.0000000	6940.000	1120197.
62.00000	.0000000	.0000000	6938.000	1179325.
64.00000	.0000000	.0000000	6936.000	1245024.
66.00000	.0000000	.0000000	6934.000	1318451.
68.00000	.0000000	.0000000	6932.000	1401056.
70.00000	.0000000	.0000000	00	1494676.
72.00000	.0000000	.0000000	6928.000	1601671.
74.00000	.0000000	.0000000	6926.000	1725126.
76.00000	.0000000	.0000000	6924.000	1869156.
78.00000	.0000000	.0000000	6922.000	2039375.
80.00000	.0000000	.0000000	6920.000	2243637.
82.00000	.0000000	.0000000	6918.000	2493291.
84.00000	.0000000	.0000000	6916.000	2805358.
86.00000	.0000000	.0000000	6914.000	3206588.
88.00000	.0000000	.0000000	6912.000	3741561.
90.00000	.0000000	.0000000	6910.000	4490523.
92.00000	.0000000	.0000000	6908.000	5613967.
94.00000	.0000000	.0000000	6906.000	7486374.
96.00000	.0000000	.0000000	6904.000	0.1123119E+08
98.00000	.0000000	.0000000	6902.000	0.2246605E+08
100.0000	.0000000	.0000000	6900.000	0.4514215E+08

C.1.3 Total Induced Voltage for the 2m Conductor-Plane Gap

Distance	X-Coord.	Y-Coord.	Z-Coord.	Value
.0000000	.0000000	.0000000	2000.000	135904.0
4.000000	.0000000	.0000000	1996.000	144791.2
8.000000	.0000000	.0000000	1992.000	152730.1
12.00000	.0000000	.0000000	1988.000	160367.1
16.00000	.0000000	.0000000	1984.000	167822.1
20.00000	.0000000	.0000000	1980.000	175218.6
24.00000	.0000000	.0000000	1976.000	182639.6
28.00000	.0000000	.0000000	1972.000	190146.5
32.00000	.0000000	.0000000	1968.000	197790.0
36.00000	.0000000	.0000000	1964.000	205615.4
40.00000	.0000000	.0000000	1960.000	213663.9
44.00000	.0000000	.0000000	1956.000	221976.2
48.00000	.0000000	.0000000	1952.000	230591.7
52.00000	.0000000	.0000000	1948.000	239550.7
56.00000	.0000000	.0000000	1944.000	248895.4
60.00000	.0000000	.0000000	1940.000	258670.2
64.00000	.0000000	.0000000	1936.000	268923.2
68.00000	.0000000	.0000000	1932.000	279706.7
72.00000	.0000000	.0000000	1928.000	291078.4
76.00000	.0000000	.0000000	1924.000	303102.3
80.00000	.0000000	.0000000	1920.000	315850.0
84.00000	.0000000	.0000000	1916.000	329402.2
88.00000	.0000000	.0000000	1912.000	343850.6
92.00000	.0000000	.0000000	1908.000	359299.5
96.00000	.0000000	.0000000	1904.000	375869.1
100.0000	.0000000	.0000000	1900.000	393698.2
104.0000	.0000000	.0000000	1896.000	412948.1
Distance	**X-Coord.**	**Y-Coord.**	**Z-Coord.**	**Value**
108.0000	.0000000	.0000000	1892.000	433808.2

112.0000	.0000000	.0000000	1888.000	456501.5
116.0000	.0000000	.0000000	1884.000	481293.5
120.0000	.0000000	.0000000	1880.000	508502.2
124.0000	.0000000	.0000000	1876.000	538512.6
128.0000	.0000000	.0000000	1872.000	571794.7
132.0000	.0000000	.0000000	1868.000	608928.9
136.0000	.0000000	.0000000	1864.000	650640.5
140.0000	.0000000	.0000000	1860.000	697848.0
144.0000	.0000000	.0000000	1856.000	751732.0
148.0000	.0000000	.0000000	1852.000	813836.3
152.0000	.0000000	.0000000	1848.000	886218.9
156.0000	.0000000	.0000000	1844.000	971686.1
160.0000	.0000000	.0000000	1840.000	1074166.
164.0000	.0000000	.0000000	1836.000	1199334.
168.0000	.0000000	.0000000	1832.000	1355701.
172.0000	.0000000	.0000000	1828.000	1556641.
176.0000	.0000000	.0000000	1824.000	1824445.
180.0000	.0000000	.0000000	1820.000	2199237.
184.0000	.0000000	.0000000	1816.000	2761263.
188.0000	.0000000	.0000000	1812.000	3697764.
192.0000	.0000000	.0000000	1808.000	5570461.
196.0000	.0000000	.0000000	1804.000	0.1118797E+08
200.0000	.0000000	.0000000	1800.000	0.4509915E+08

C.1.4 Total Induced Voltage for the 6m Conductor-Plane Gap

Distance	X-Coord.	Y-Coord.	Z-Coord.	Value
.0000000	.0000000	.0000000	6000.000	137165.0
4.000000	.0000000	.0000000	5996.000	146219.6
8.000000	.0000000	.0000000	5992.000	154287.2
12.00000	.0000000	.0000000	5988.000	162035.0
16.00000	.0000000	.0000000	5984.000	169586..
20.00000	.0000000	.0000000	5980.000	177068.3
24.00000	.0000000	.0000000	5976.000	184566.5
28.00000	.0000000	.0000000	5972.000	192143.8
32.00000	.0000000	.0000000	5968.000	199852.2
36.00000	.0000000	.0000000	5964.000	207737.7
40.00000	.0000000	.0000000	5960.000	215842.5
44.00000	.0000000	.0000000	5956.000	224207.5
48.00000	.0000000	.0000000	5952.000	232872.8
52.00000	.0000000	.0000000	5948.000	241879.1
56.00000	.0000000	.0000000	5944.000	251268.6
60.00000	.0000000	.0000000	5940.000	261086.2
64.00000	.0000000	.0000000	5936.000	271380.2
68.00000	.0000000	.0000000	5932.000	282203.1
72.00000	.0000000	.0000000	5928.000	293612.7
76.00000	.0000000	.0000000	5924.000	305673.1
80.00000	.0000000	.0000000	5920.000	318456.1
84.00000	.0000000	.0000000	5916.000	332042.5
88.00000	.0000000	.0000000	5912.000	346524.0
92.00000	.0000000	.0000000	5908.000	362005.0
96.00000	.0000000	.0000000	5904.000	378605.9
100.0000	.0000000	.0000000	5900.000	396465.3
104.0000	.0000000	.0000000	5896.000	415745.0

Distance	X-Coord.	Y-Coord.	Z-Coord.	Value
108.0000	.0000000	.0000000	5892.000	436633.9
112.0000	.0000000	.0000000	5888.000	459355.5
116.0000	.0000000	.0000000	5884.000	484175.1
120.0000	.0000000	.0000000	5880.000	511410.9
124.0000	.0000000	.0000000	5876.000	541447.8
128.0000	.0000000	.0000000	5872.000	574755.8
132.0000	.0000000	.0000000	5868.000	611915.5
136.0000	.0000000	.0000000	5864.000	653652.1
140.0000	.0000000	.0000000	5860.000	700884.1
144.0000	.0000000	.0000000	5856.000	754792.3
148.0000	.0000000	.0000000	5852.000	816920.3
152.0000	.0000000	.0000000	5848.000	889326.3
156.0000	.0000000	.0000000	5844.000	974816.6
160.0000	.0000000	.0000000	5840.000	1077320.
164.0000	.0000000	.0000000	5836.000	1202510.
168.0000	.0000000	.0000000	5832.000	1358898.
172.0000	.0000000	.0000000	5828.000	1559860.
176.0000	.0000000	.0000000	5824.000	1827686.
180.0000	.0000000	.0000000	5820.000	2202499.
184.0000	.0000000	.0000000	5816.000	2764546.
188.0000	.0000000	.0000000	5812.000	3701067.
192.0000	.0000000	.0000000	5808.000	5573785.
196.0000	.0000000	.0000000	5804.000	0.1119131E+08
200.0000	.0000000	.0000000	5800.000	0.4510251E+08

C.1.5 Total Induced Voltage for the 5m Tower-Conductor Gap

Distance	X-Coord.	Y-Coord.	Z-Coord.	Value
.0000000	.0000000	16.00000	10016.00	16722.50
4.000000	.0000000	20.00000	10016.00	18768.18
8.000000	.0000000	24.00000	10016.00	20501.88
12.00000	.0000000	28.00000	10016.00	22121.29
16.00000	.0000000	32.00000	10016.00	23657.96
20.00000	.0000000	36.00000	10016.00	25144.01
24.00000	.0000000	40.00000	10016.00	26600.53
28.00000	.0000000	44.00000	10016.00	28043.15
32.00000	.0000000	48.00000	10016.00	29484.97
36.00000	.0000000	52.00000	10016.00	30938.00
40.00000	.0000000	56.00000	10016.00	32413.70
44.00000	.0000000	60.00000	10016.00	33924.22
48.00000	.0000000	64.00000	10016.00	35482.10
52.00000	.0000000	68.00000	10016.00	37101.00
56.00000	.0000000	72.00000	10016.00	38796.14
60.00000	.0000000	76.00000	10016.00	40584.85
64.00000	.0000000	80.00000	10016.00	42496.87
68.00000	.0000000	84.00000	10016.00	44535.09
72.00000	.0000000	88.00000	10016.00	46736.39
76.00000	.0000000	92.00000	10016.00	49132.01
80.00000	.0000000	96.00000	10016.00	51758.59
84.00000	.0000000	100.0000	10016.00	54659.25
88.00000	.0000000	104.0000	10016.00	57884.91
92.00000	.0000000	108.0000	10016.00	61495.86
96.00000	.0000000	112.0000	10016.00	65563.70
100.0000	.0000000	116.0000	10016.00	70173.80
104.0000	.0000000	120.0000	10016.00	75428.25

Distance	X-Coord.	Y-Coord.	Z-Coord.	Value
108.0000	.0000000	124.0000	10016.00	81449.69
112.0000	.0000000	128.0000	10016.00	88386.10
116.0000	.0000000	132.0000	10016.00	96416.89
120.0000	.0000000	136.0000	10016.00	105760.9
124.0000	.0000000	140.0000	10016.00	116686.4
128.0000	.0000000	144.0000	10016.00	129524.8
[illegible]	[illegible]	148.0000	10016.00	144688.3
[illegible]	[illegible]	152.0000	10016.00	162693.0
140.0000	[illegible]	156.0000	10016.00	184790.1
[illegible]	[illegible]	160.0000	10016.00	210004.9
148.0000	.0000000	164.0000	10016.00	241184.9
152.0000	.0000000	168.0000	10016.00	279041.1
156.0000	.0000000	172.0000	10016.00	325111.2
160.0000	.0000000	176.0000	10016.00	380596.6
164.0000	.0000000	180.0000	10016.00	444073.8
168.0000	.0000000	184.0000	10016.00	609240.9
172.0000	.0000000	188.0000	10016.00	828177.4
176.0000	.0000000	192.0000	10016.00	1116925.
180.0000	.0000000	196.0000	10016.00	1513796.
184.0000	.0000000	200.0000	10016.00	2098195.
188.0000	.0000000	204.0000	10016.00	3056893.
192.0000	.0000000	208.0000	10016.00	4951202.
196.0000	.0000000	212.0000	10016.00	0.1058893E+08
200.0000	.0000000	216.0000	10016.00	0.4452422E+08

C.1.6 Total Induced Voltage for the 9.3m Tower-Conductor Gap

Distance	X-Coord.	Y-Coord.	Z-Coord.	Value
.0000000	.0000000	16.00000	15016.00	18082.87
4.000000	.0000000	20.00000	15016.00	19872.34
8.000000	.0000000	24.00000	15016.00	21375.09
12.00000	.0000000	28.00000	15016.00	22772.82
16.00000	.0000000	32.00000	15016.00	24095.08
20.00000	.0000000	36.00000	15016.00	25372.10
24.00000	.0000000	40.00000	15016.00	26624.14
28.00000	.0000000	44.00000	15016.00	27866.53
32.00000	.0000000	48.00000	15016.00	29112.43
36.00000	.0000000	52.00000	15016.00	30374.15
40.00000	.0000000	56.00000	15016.00	31663.76
44.00000	.0000000	60.00000	15016.00	32994.17
48.00000	.0000000	64.00000	15016.00	34379.00
52.00000	.0000000	68.00000	15016.00	35833.21
56.00000	.0000000	72.00000	15016.00	37376.79
60.00000	.0000000	76.00000	15016.00	39022.64
64.00000	.0000000	80.00000	15016.00	40800.54
68.00000	.0000000	84.00000	15016.00	42727.45
72.00000	.0000000	88.00000	15016.00	44837.80
76.00000	.0000000	92.00000	15016.00	47166.69
80.00000	.0000000	96.00000	15016.00	49755.32
84.00000	.0000000	100.0000	15016.00	52652.17
88.00000	.0000000	104.0000	15016.00	55914.49
92.00000	.0000000	108.0000	15016.00	59610.03
96.00000	.0000000	112.0000	15016.00	63819.28
100.0000	.0000000	116.0000	15016.00	68638.13
104.0000	.0000000	120.0000	15016.00	74181.25

Distance	X-Coord.	Y-Coord.	Z-Coord.	Value
108.0000	.0000000	124.0000	15016.00	80586.40
112.0000	.0000000	128.0000	15016.00	88019.81
116.0000	.0000000	132.0000	15016.00	96683.19
120.0000	.0000000	136.0000	15016.00	106822.7
124.0000	.0000000	140.0000	15016.00	118740.9
128.0000	.0000000	144.0000	15016.00	132812.2
132.0000	.0000000	148.0000	15016.00	149504.4
136.0000	.0000000	152.0000	15016.00	169406.6
140.0000	.0000000	156.0000	15016.00	193268.6
144.0000	.0000000	160.0000	15016.00	222065.0
148.0000	.0000000	164.0000	15016.00	257028.7
152.0000	.0000000	168.0000	15016.00	299809.8
156.0000	.0000000	172.0000	15016.00	352537.8
160.0000	.0000000	176.0000	15016.00	417749.8
164.0000	.0000000	180.0000	15016.00	500805.6
168.0000	.0000000	184.0000	15016.00	675255.4
172.0000	.0000000	188.0000	15016.00	895758.9
176.0000	.0000000	192.0000	15016.00	1183551.
180.0000	.0000000	196.0000	15016.00	1578155.
184.0000	.0000000	200.0000	15016.00	2159546.
188.0000	.0000000	204.0000	15016.00	3114793.
192.0000	.0000000	208.0000	15016.00	5005408.
196.0000	.0000000	212.0000	15016.00	0.1063932E+08
200.0000	.0000000	216.0000	15016.00	0.4457077E+08

C.2.1 Changing the Value of 's'

Distance	X-Coord.	Y-Coord.	Z-Coord.	Value
.0000000	.0000000	.0000000	7000.000	221432.5
4.000000	.0000000	.0000000	6996.000	226017.0
8.000000	.0000000	.0000000	6992.000	230792.6
12.00000	.0000000	.0000000	6988.000	235771.5
16.00000	.0000000	.0000000	6984.000	240966.9
20.00000	.0000000	.0000000	6980.000	246393.2
24.00000	.0000000	.0000000	6976.000	252066.2
28.00000	.0000000	.0000000	6972.000	258003.1
32.00000	.0000000	.0000000	6968.000	264222.8
36.00000	.0000000	.0000000	6964.000	270745.9
40.00000	.0000000	.0000000	6960.000	277595.2
44.00000	.0000000	.0000000	6956.000	284795.9
48.00000	.0000000	.0000000	6952.000	292375.5
52.00000	.0000000	.0000000	6948.000	300364.9
56.00000	.0000000	.0000000	6944.000	308798.2
60.00000	.0000000	.0000000	6940.000	317713.5
64.00000	.0000000	.0000000	6936.000	327153.3
68.00000	.0000000	.0000000	6932.000	337165.2
72.00000	.0000000	.0000000	6928.000	347802.9
76.00000	.0000000	.0000000	6924.000	359127.0
80.00000	.0000000	.0000000	6920.000	371206.1
84.00000	.0000000	.0000000	6916.000	384118.3
88.00000	.0000000	.0000000	6912.000	397952.8
92.00000	.0000000	.0000000	6908.000	412812.3
96.00000	.0000000	.0000000	6904.000	428814.8
100.0000	.0000000	.0000000	6900.000	446097.6
104.0000	.0000000	.0000000	6896.000	464820.7

Distance	X-Coord.	Y-Coord.	Z-Coord.	Value
108.0000	.0000000	.0000000	6892.000	485172.0
112.0000	.0000000	.0000000	6888.000	507373.5
116.0000	.0000000	.0000000	6884.000	531689.5
120.0000	.0000000	.0000000	6880.000	558437.2
124.0000	.0000000	.0000000	6876.000	588000.6
128.0000	.0000000	.0000000	6872.000	620848.9
132.0000	.0000000	.0000000	6868.000	657561.8
136.0000	.0000000	.0000000	6864.000	698863.9
140.0000	.0000000	.0000000	6860.000	745673.1
144.0000	.0000000	.0000000	6856.000	799169.5
148.0000	.0000000	.0000000	6852.000	860896.2
152.0000	.0000000	.0000000	6848.000	932910.9
156.0000	.0000000	.0000000	6844.000	1018019.
160.0000	.0000000	.0000000	6840.000	1120150.
164.0000	.0000000	.0000000	6836.000	1244976.
168.0000	.0000000	.0000000	6832.000	1401009.
172.0000	.0000000	.0000000	6828.000	1601623.
176.0000	.0000000	.0000000	6824.000	1869109.
180.0000	.0000000	.0000000	6820.000	2243589.
184.0000	.0000000	.0000000	6816.000	2805310.
188.0000	.0000000	.0000000	6812.000	3741513.
192.0000	.0000000	.0000000	6808.000	5613919.
196.0000	.0000000	.0000000	6804.000	0.1123115E+08
200.0000	.0000000	.0000000	6800.000	0.4514210E+08

C.2.2 Changing the Magnitude of Q_o

Distance	X-Coord.	Y-Coord.	Z-Coord.	Value
.0000000	.0000000	.0000000	7000.000	446.1448
2.000000	.0000000	.0000000	6998.000	455.3153
4.000000	.0000000	.0000000	6996.000	464.8679
6.000000	.0000000	.0000000	6994.000	474.8271
8.000000	.0000000	.0000000	6992.000	485.2192
10.00000	.0000000	.0000000	6990.000	496.0733
12.00000	.0000000	.0000000	6988.000	507.4208
14.00000	.0000000	.0000000	6986.000	519.2960
16.00000	.0000000	.0000000	6984.000	531.7368
18.00000	.0000000	.0000000	6982.000	544.7845
20.00000	.0000000	.0000000	6980.000	558.4845
22.00000	.0000000	.0000000	6978.000	572.8872
24.00000	.0000000	.0000000	6976.000	588.0479
26.00000	.0000000	.0000000	6974.000	604.0282
28.00000	.0000000	.0000000	6972.000	620.8963
30.00000	.0000000	.0000000	6970.000	638.7282
32.00000	.0000000	.0000000	6968.000	657.6092
34.00000	.0000000	.0000000	6966.000	677.6345
36.00000	.0000000	.0000000	6964.000	698.9113
38.00000	.0000000	.0000000	6962.000	721.5610
40.00000	.0000000	.0000000	6960.000	745.7206
42.00000	.0000000	.0000000	6958.000	771.5464
44.00000	.0000000	.0000000	6956.000	799.2170
46.00000	.0000000	.0000000	6954.000	828.9373
48.00000	.0000000	.0000000	6952.000	860.9438
50.00000	.0000000	.0000000	6950.000	895.5108
52.00000	.0000000	.0000000	6948.000	932.9585

Distance	X-Coord.	Y-Coord.	Z-Coord.	Value
54.00000	.0000000	.0000000	6946.000	973.6625
56.00000	.0000000	.0000000	6944.000	1018.067
58.00000	.0000000	.0000000	6942.000	1066.700
60.00000	.0000000	.0000000	6940.000	1120.197
62.00000	.0000000	.0000000	6938.000	1179.326
64.00000	.0000000	.0000000	6936.000	1245.024
66.00000	.0000000	.0000000	6934.000	1318.451
68.00000	.0000000	.0000000	6932.000	1401.057
70.00000	.0000000	.0000000	6930.000	1494.676
72.00000	.0000000	.0000000	6928.000	1601.671
74.00000	.0000000	.0000000	6926.000	1725.126
76.00000	.0000000	.0000000	6924.000	1869.156
78.00000	.0000000	.0000000	6922.000	2039.375
80.00000	.0000000	.0000000	6920.000	2243.637
82.00000	.0000000	.0000000	6918.000	2493.291
84.00000	.0000000	.0000000	6916.000	2805.358
86.00000	.0000000	.0000000	6914.000	3206.588
88.00000	.0000000	.0000000	6912.000	3741.561
90.00000	.0000000	.0000000	6910.000	4490.523
92.00000	.0000000	.0000000	6908.000	5613.967
94.00000	.0000000	.0000000	6906.000	7486.374
96.00000	.0000000	.0000000	6904.000	11231.19
98.00000	.0000000	.0000000	6902.000	22466.05
100.0000	.0000000	.0000000	6900.000	45142.15

C.2.3 Changing the Space Charge Radius

Distance	X-Coord.	Y-Coord.	Z-Coord.	Value
.0000000	.0000000	.0000000	7000.000	446144.8
2.000000	.0000000	.0000000	6998.000	455315.3
4.000000	.0000000	.0000000	6996.000	464867.9
6.000000	.0000000	.0000000	6994.000	474827.1
8.000000	.0000000	.0000000	6992.000	485219.2
10.00000	.0000000	.0000000	6990.000	496073.3
12.00000	.0000000	.0000000	6988.000	507420.8
14.00000	.0000000	.0000000	6986.000	519296.0
16.00000	.0000000	.0000000	6984.000	531736.8
18.00000	.0000000	.0000000	6982.000	544784.5
20.00000	.0000000	.0000000	6980.000	558484.6
22.00000	.0000000	.0000000	6978.000	572887.2
24.00000	.0000000	.0000000	6976.000	588048.0
26.00000	.0000000	.0000000	6974.000	604028.2
28.00000	.0000000	.0000000	6972.000	620896.3
30.00000	.0000000	.0000000	6970.000	638728.3
32.00000	.0000000	.0000000	6968.000	657609.2
34.00000	.0000000	.0000000	6966.000	677634.5
36.00000	.0000000	.0000000	6964.000	698911.4
38.00000	.0000000	.0000000	6962.000	721561.0
40.00000	.0000000	.0000000	6960.000	745720.7
42.00000	.0000000	.0000000	6958.000	771546.5
44.00000	.0000000	.0000000	6956.000	799217.1
46.00000	.0000000	.0000000	6954.000	828937.4
48.00000	.0000000	.0000000	6952.000	860943.9
50.00000	.0000000	.0000000	6950.000	895511.0
52.00000	.0000000	.0000000	6948.000	932958.7

Distance	X-Coord.	Y-Coord.	Z-Coord.	Value
54.00000	.0000000	.0000000	6946.000	973662.8
56.00000	.0000000	.0000000	6944.000	1018067.
58.00000	.0000000	.0000000	6942.000	1066701.
60.00000	.0000000	.0000000	6940.000	1120198.
62.00000	.0000000	.0000000	6938.000	1179326.
64.00000	.0000000	.0000000	6936.000	1245025.
66.00000	.0000000	.0000000	6934.000	1318452.
68.00000	.0000000	.0000000	6932.000	1401058.
70.00000	.0000000	.0000000	6930.000	1494679.
72.00000	.0000000	.0000000	6928.000	1601675.
74.00000	.0000000	.0000000	6926.000	1725132.
76.00000	.0000000	.0000000	6924.000	1869168.
78.00000	.0000000	.0000000	6922.000	2039396.
80.00000	.0000000	.0000000	6920.000	2243679.
82.00000	.0000000	.0000000	6918.000	2495385.
84.00000	.0000000	.0000000	6916.000	2805601.
86.00000	.0000000	.0000000	6914.000	3207316.
88.00000	.0000000	.0000000	6912.000	3744184.
90.00000	.0000000	.0000000	6910.000	4502622.
92.00000	.0000000	.0000000	6908.000	4509588.
94.00000	.0000000	.0000000	6906.000	4511078.
96.00000	.0000000	.0000000	6904.000	4511271.
98.00000	.0000000	.0000000	6902.000	4511284
100.0000	.0000000	.0000000	6900.000	4511284.

C.3.1 Changing the Space Charge Position

Distance	X-Coord.	Y-Coord.	Z-Coord.	Value
.0000000	.0000000	.0000000	6000.000	343936.7
2.000000	.0000000	.0000000	5998.000	356530.1
4.000000	.0000000	.0000000	5996.000	368157.2
6.000000	.0000000	.0000000	5994.000	380208.2
8.000000	.0000000	.0000000	5992.000	392539.4
10.00000	.0000000	.0000000	5990.000	405162.1
12.00000	.0000000	.0000000	5988.000	418128.6
14.00000	.0000000	.0000000	5986.000	431497.3
16.00000	.0000000	.0000000	5984.000	445325.3
18.00000	.0000000	.0000000	5982.000	459669.2
20.00000	.0000000	.0000000	5980.000	474585.9
22.00000	.0000000	.0000000	5978.000	490135.1
24.00000	.0000000	.0000000	5976.000	506379.7
26.00000	.0000000	.0000000	5974.000	523387.5
28.00000	.0000000	.0000000	5972.000	541232.1
30.00000	.0000000	.0000000	5970.000	559994.4
32.00000	.0000000	.0000000	5968.000	579763.5
34.00000	.0000000	.0000000	5966.000	600638.5
36.00000	.0000000	.0000000	5964.000	622729.7
38.00000	.0000000	.0000000	5962.000	646160.8
40.00000	.0000000	.0000000	5960.000	671071.9
42.00000	.0000000	.0000000	5958.000	697621.4
44.00000	.0000000	.0000000	5956.000	725989.9
46.00000	.0000000	.0000000	5954.000	756384.1
48.00000	.0000000	.0000000	5952.000	789042.0
50.00000	.0000000	.0000000	5950.000	824239.5
52.00000	.0000000	.0000000	5948.000	862298.0

Distance	X-Coord.	Y-Coord.	Z-Coord.	Value
54.00000	.0000000	.0000000	5946.000	903594.2
56.00000	.0000000	.0000000	5944.000	948573.5
58.00000	.0000000	.0000000	5942.000	997765.4
60.00000	.0000000	.0000000	5940.000	1051805.
62.00000	.0000000	.0000000	5938.000	1111461.
64.00000	.0000000	.0000000	5936.000	1177674.
66.00000	.0000000	.0000000	5934.000	1251602.
68.00000	.0000000	.0000000	5932.000	1334696.
70.00000	.0000000	.0000000	5930.000	1428792.
72.00000	.0000000	.0000000	5928.000	1536251.
74.00000	.0000000	.0000000	5926.000	1660161.
76.00000	.0000000	.0000000	5924.000	1804635.
78.00000	.0000000	.0000000	5922.000	1975287.
80.00000	.0000000	.0000000	5920.000	2179973.
82.00000	.0000000	.0000000	5918.000	2430042.
84.00000	.0000000	.0000000	5916.000	2742515.
86.00000	.0000000	.0000000	5914.000	3144142.
88.00000	.0000000	.0000000	5912.000	3679504.
90.00000	.0000000	.0000000	5910.000	4428847.
92.00000	.0000000	.0000000	5908.000	5552663.
94.00000	.0000000	.0000000	5906.000	7425433.
96.00000	.0000000	.0000000	5904.000	0.1117060E+08
98.00000	.0000000	.0000000	5902.000	0.2240580E+08
100.0000	.0000000	.0000000	5900.000	0.4508208E+08

C.3.2 Changing the Conductor Radius

Distance	X-Coord.	Y-Coord.	Z-Coord.	Value
.0000000	.0000000	.0000000	6000.000	132541.4
4.000000	.0000000	.0000000	5996.000	145781.1
8.000000	.0000000	.0000000	5992.000	155604.0
12.00000	.0000000	.0000000	5988.000	164362.1
16.00000	.0000000	.0000000	5984.000	172536.5
20.00000	.0000000	.0000000	5980.000	180430.5
24.00000	.0000000	.0000000	5976.000	188212.5
28.00000	.0000000	.0000000	5972.000	195989.7
32.00000	.0000000	.0000000	5968.000	203840.8
36.00000	.0000000	.0000000	5964.000	211828.4
40.00000	.0000000	.0000000	5960.000	220005.9
44.00000	.0000000	.0000000	5956.000	228422.2
48.00000	.0000000	.0000000	5952.000	237122.5
52.00000	.0000000	.0000000	5948.000	246151.2
56.00000	.0000000	.0000000	5944.000	255553.5
60.00000	.0000000	.0000000	5940.000	265376.4
64.00000	.0000000	.0000000	5936.000	275669.7
68.00000	.0000000	.0000000	5932.000	286487.1
72.00000	.0000000	.0000000	5928.000	297887.3
76.00000	.0000000	.0000000	5924.000	309935.3
80.00000	.0000000	.0000000	5920.000	322703.5
84.00000	.0000000	.0000000	5916.000	336273.0
88.00000	.0000000	.0000000	5912.000	350735.9
92.00000	.0000000	.0000000	5908.000	366197.2
96.00000	.0000000	.0000000	5904.000	382777.2
100.0000	.0000000	.0000000	5900.000	400615.0
104.0000	.0000000	.0000000	5896.000	419872.3

Distance	X-Coord.	Y-Coord.	Z-Coord.	Value
108.0000	.0000000	.0000000	5892.000	440738.4
112.0000	.0000000	.0000000	5888.000	463436.8
116.0000	.0000000	.0000000	5884.000	488232.9
120.0000	.0000000	.0000000	5880.000	515444.9
124.0000	.0000000	.0000000	5876.000	545457.9
128.0000	.0000000	.0000000	5872.000	578742.0
132.0000	.0000000	.0000000	5868.000	615877.7
136.0000	.0000000	.0000000	5864.000	657590.3
140.0000	.0000000	.0000000	5860.000	704798.4
144.0000	.0000000	.0000000	5856.000	758682.8
148.0000	.0000000	.0000000	5852.000	820787.1
152.0000	.0000000	.0000000	5848.000	893169.4
156.0000	.0000000	.0000000	5844.000	978636.2
160.0000	.0000000	.0000000	5840.000	1081116.
164.0000	.0000000	.0000000	5836.000	1206283.
168.0000	.0000000	.0000000	5832.000	1362649.
172.0000	.0000000	.0000000	5828.000	1563585.
176.0000	.0000000	.0000000	5824.000	1831391.
180.0000	.0000000	.0000000	5820.000	2206182.
184.0000	.0000000	.0000000	5816.000	2768706.
188.0000	.0000000	.0000000	5812.000	3704706.
192.0000	.0000000	.0000000	5808.000	5577401.
196.0000	.0000000	.0000000	5804.000	0.1119491E+08
200.0000	.0000000	.0000000	5800.000	0.2510609E+08

C.3.3 The Conductor-Bundle to Plane Gap

Distance	X-Coord.	Y-Coord.	Z-Coord.	Value
.0000000	.0000000	.0000000	6000.000	18318.86
16.00000	.0000000	.0000000	5984.000	20038.07
32.00000	.0000000	.0000000	5968.000	21975.73
48.00000	.0000000	.0000000	5952.000	24065.82
64.00000	.0000000	.0000000	5936.000	26240.23
80.00000	.0000000	.0000000	5920.000	28474.18
96.00000	.0000000	.0000000	5904.000	30745.85
112.0000	.0000000	.0000000	5888.000	33047.54
128.0000	.0000000	.0000000	5872.000	35379.08
144.0000	.0000000	.0000000	5856.000	37744.72
160.0000	.0000000	.0000000	5840.000	40166.18
176.0000	.0000000	.0000000	5824.000	42638.28
192.0000	.0000000	.0000000	5808.000	45171.78
208.0000	.0000000	.0000000	5792.000	47775.73
224.0000	.0000000	.0000000	5776.000	50439.17
240.0000	.0000000	.0000000	5760.000	53194.96
256.0000	.0000000	.0000000	5744.000	56055.99
272.0000	.0000000	.0000000	5728.000	59036.21
288.0000	.0000000	.0000000	5712.000	62150.88
304.0000	.0000000	.0000000	5696.000	65416.80
320.0000	.0000000	.0000000	5680.000	68852.63
336.0000	.0000000	.0000000	5664.000	72479.26
352.0000	.0000000	.0000000	5648.000	76320.22
368.0000	.0000000	.0000000	5632.000	80402.25
384.0000	.0000000	.0000000	5616.000	84755.90
400.0000	.0000000	.0000000	5600.000	89416.39
416.0000	.0000000	.0000000	5584.000	94424.54

Distance	X-Coord.	Y-Coord.	Z-Coord.	Value
432.0000	.0000000	.0000000	5568.000	99828.09
448.0000	.0000000	.0000000	5552.000	105683.2
464.0000	.0000000	.0000000	5536.000	112056.6
480.0000	.0000000	.0000000	5520.000	119028.2
496.0000	.0000000	.0000000	5504.000	126694.5
512.0000	.0000000	.0000000	5488.000	135173.3
528.0000	.0000000	.0000000	5472.000	144610.0
544.0000	.0000000	.0000000	5456.000	155186.1
560.0000	.0000000	.0000000	5440.000	167131.5
576.0000	.0000000	.0000000	5424.000	180741.5
592.0000	.0000000	.0000000	5408.000	196402.4
608.0000	.0000000	.0000000	5392.000	214628.8
624.0000	.0000000	.0000000	5376.000	236122.4
640.0000	.0000000	.0000000	5360.000	261865.5
656.0000	.0000000	.0000000	5344.000	293276.9
672.0000	.0000000	.0000000	5328.000	332484.4
688.0000	.0000000	.0000000	5312.000	382845.1
704.0000	.0000000	.0000000	5296.000	449915.8
720.0000	.0000000	.0000000	5280.000	543726.6
736.0000	.0000000	.0000000	5264.000	684339.9
752.0000	.0000000	.0000000	5248.000	918560.5
768.0000	.0000000	.0000000	5232.000	1386824.
784.0000	.0000000	.0000000	5216.000	2791272.
800.0000	.0000000	.0000000	5200.000	0.4512719E+08

C.4.1 The Tower Window Structure with Three Planes

Distance	X-Coord.	Y-Coord.	Z-Coord.	Value
.0000000	.0000000	16.00000	10016.00	18361.82
4.000000	.0000000	20.00000	10016.00	20424.03
8.000000	.0000000	24.00000	10016.00	22176.60
12.00000	.0000000	28.00000	10016.00	23819.41
16.00000	.0000000	32.00000	10016.00	25378.27
20.00000	.0000000	36.00000	10016.00	26887.91
24.00000	.0000000	40.00000	10016.00	28369.22
28.00000	.0000000	44.00000	10016.00	29837.56
32.00000	.0000000	48.00000	10016.00	31305.68
36.00000	.0000000	52.00000	10016.00	32785.09
40.00000	.0000000	56.00000	10016.00	34286.69
44.00000	.0000000	60.00000	10016.00	35821.86
48.00000	.0000000	64.00000	10016.00	37402.26
52.00000	.0000000	68.00000	10016.00	39040.39
56.00000	.0000000	72.00000	10016.00	40750.17
60.00000	.0000000	76.00000	10016.00	42547.26
64.00000	.0000000	80.00000	10016.00	44449.57
68.00000	.0000000	84.00000	10016.00	46477.72
72.00000	.0000000	88.00000	10016.00	48655.67
76.00000	.0000000	92.00000	10016.00	51011.33
80.00000	.0000000	96.00000	10016.00	53577.41
84.00000	.0000000	100.0000	10016.00	56392.35
88.00000	.0000000	104.0000	10016.00	59501.51
92.00000	.0000000	108.0000	10016.00	62958.52
96.00000	.0000000	112.0000	10016.00	66841.43
100.0000	.0000000	116.0000	10016.00	71200.27
104.0000	.0000000	120.0000	10016.00	76137.19

Distance	X-Coord.	Y-Coord.	Z-Coord.	Value
108.0000	.0000000	124.0000	10016.00	81760.95
112.0000	.0000000	128.0000	10016.00	88202.60
116.0000	.0000000	132.0000	10016.00	95620.81
120.0000	.0000000	136.0000	10016.00	104208.6
124.0000	.0000000	140.0000	10016.00	114[illegible]2.2
128.0000	.0000000	144.0000	10016.00	125892.0
132.0000	.0000000	148.0000	10016.00	139637.1
136.0000	.0000000	152.0000	10016.00	155883.6
140.0000	.0000000	156.0000	10016.00	175187.2
144.0000	.0000000	160.0000	10016.00	198239.1
148.0000	.0000000	164.0000	10016.00	225886.6
152.0000	.0000000	168.0000	10016.00	259120.9
156.0000	.0000000	172.0000	10016.00	298862.6
160.0000	.0000000	176.0000	10016.00	345084.0
164.0000	.0000000	180.0000	10016.00	389841.6
168.0000	.0000000	184.0000	10016.00	548814.2
172.0000	.0000000	188.0000	10016.00	768549.4
176.0000	.0000000	192.0000	10016.00	1060223.
180.0000	.0000000	196.0000	10016.00	1461003.
184.0000	.0000000	200.0000	10016.00	2049783.
188.0000	.0000000	204.0000	10016.00	3013039.
192.0000	.0000000	208.0000	10016.00	4911918.
196.0000	.0000000	212.0000	10016.00	0.1055412E+08
200.0000	.0000000	216.0000	10016.00	0.4449373E+08

C.4.2 The Tower-Conductor-Bundle Gap

Distance	X-Coord.	Y-Coord.	Z-Coord.	Value
.0000000	.0000000	.0000000	19041.10	959.8737
27.00000	.0000000	27.00000	19041.10	1249.027
54.00000	.0000000	54.00000	19041.10	1561.004
81.00000	.0000000	81.00000	19041.10	1901.110
108.0000	.0000000	108.0000	19041.10	2276.141
135.0000	.0000000	135.0000	19041.10	2694.515
162.0000	.0000000	162.0000	19041.10	3155.638
189.0000	.0000000	189.0000	19041.10	3657.447
216.0000	.0000000	216.0000	19041.10	4271.313
243.0000	.0000000	243.0000	19041.10	4976.217
270.0000	.0000000	270.0000	19041.10	5784.760
297.0000	.0000000	297.0000	19041.10	6695.496
324.0000	.0000000	324.0000	19041.10	7743.264
351.0000	.0000000	351.0000	19041.10	8919.039
378.0000	.0000000	378.0000	19041.10	10226.87
405.0000	.0000000	405.0000	19041.10	11726.92
432.0000	.0000000	432.0000	19041.10	13326.72
459.0000	.0000000	459.0000	19041.10	15032.43
486.0000	.0000000	486.0000	19041.10	16870.29
513.0000	.0000000	513.0000	19041.10	18825.98
540.0000	.0000000	540.0000	19041.10	20934.92
567.0000	.0000000	567.0000	19041.10	23193.07
594.0000	.0000000	594.0000	19041.10	25597.90
621.0000	.0000000	621.0000	19041.10	28165.99
648.0000	.0000000	648.0000	19041.10	30911.24
675.0000	.0000000	675.0000	19041.10	33850.99
702.0000	.0000000	702.0000	19041.10	37006.50

Distance	X-Coord.	Y-Coord.	Z-Coord.	Value
729.0000	.0000000	729.0000	19041.10	[illegible]
756.0000	.0000000	756.0000	19041.10	44068.17
783.0000	.0000000	783.0000	19041.10	48049.76
810.0000	.0000000	810.0000	19041.10	52387.99
837.0000	.0000000	837.0000	19041.10	57138.99
864.0000	.0000000	864.0000	19041.10	62371.65
891.0000	.0000000	891.0000	19041.10	68171.39
918.0000	.0000000	918.0000	19041.10	74645.19
945.0000	.0000000	945.0000	19041.10	81928.74
972.0000	.0000000	972.0000	19041.10	90196.61
999.0000	.0000000	999.0000	19041.10	99695.80
1026.000	.0000000	1026.000	19041.10	110691.8
1053.000	.0000000	1053.000	19041.10	123620.9
1080.000	.0000000	1080.000	19041.10	139064.9
1107.000	.0000000	1107.000	19041.10	157912.1
1134.000	.0000000	1134.000	19041.10	181258.3
1161.000	.0000000	1161.000	19041.10	211361.0
1188.000	.0000000	1188.000	19041.10	251262.7
1215.000	.0000000	1215.000	19041.10	307005.6
1242.000	.0000000	1242.000	19041.10	390374.9
1269.000	.0000000	1269.000	19041.10	529402.0
1296.000	.0000000	1296.000	19041.10	806982.0
1323.000	.0000000	1323.000	19041.10	1639190.
1350.000	.0000000	1350.000	19041.10	0.4512094E+08

Appendix D

In addition to the tests being performed on varying the gap distance, d, between the high voltage electrode and the ground plane, which are the most essential tests for verifying the Rizk model, other tests have also being performed to analyse the effects of changing various other parameters in the models of the rod-plane, conductor-plane and tower-conductor configurations.

In the rod-plane gap, the value of s which defines the position at which the space charge, Q_s, is positioned, is changed. In addition thereto, the effects of varying the charge magnitude as well as the radius of the space charge are examined.

Changes that are made in the conductor-plane model also examine the influence of changing the space charge position as well as how varying the radius of the conductor influences the breakdown voltage. The feasibility of using conductor-bundles as opposed to single conductors is tested.

Two additional tests have been done on the tower-conductor model. Firstly, the tower window structure is changed from a square setup with four sides to a square setup with three sides - two side planes and a top plane. Secondly, a test is carried out using a tower-conductor-bundle where the tower window has three sides as described above.

In the following sections, the total induced voltage for each of the tests will be taken from the results given in the listed sections of *Appendix C*. The procedure for calculating the continuous leader inception voltage from the total induced voltage as well as the leader voltage drop and the 50% breakdown voltage will not be discussed as it has already been dealt with in *Chapter 3*, *Chapter 4* and *Chapter 5* for the rod-plane, conductor-plane and tower-conductor gaps respectively.

D.1.1 Changing the Value of 's' in the Rod-Plane Model

The magnitude of *s* was increased from 100mm between the rod tip and the centre of the space charge to 200mm. The gap length between the rod tip and the plane was 7m. The results for the total induced voltage measured between the rod tip and the centre of the space charge are listed in *Appendix C.2.1*.

The total induced voltage measured at a distance 80mm from the centre of the space charge is 5584kV. The continuous leader inception voltage is calculated to be 963.8kV. The leader voltage drop is equal to 302.9kV and the 50% breakdown voltage is 1490kV.

This value for the 50% breakdown voltage is compared with that obtained in section *3.3 The Breakdown Voltage*, where the breakdown voltage obtained for a 7m rod-plane gap with the space charge at a distance 100mm from the rod tip is 1496kV. The measured value for the breakdown voltage is 1555kV and hence it can be concluded that moving the space charge further away from the rod tip reduces the accuracy of the charge simulation method.

D.1.2 Changing the Magnitude of Q_o in the Rod-Plane Model

The magnitude of the space charge, Q_o, is changed to investigate if it has any effect on the results of the charge simulation method. The gap between the rod tip and the plane is maintained at 7m and the space charge is positioned at a distance 100mm from the rod tip. Hence the results can be compared with that obtained for a 7m rod-plane gap in *Chapter 3*. The space charge is given a new value of 5nC and the results for the total induced voltage are given in *Appendix C.2.2*.

The total induced voltage measured at a distance 80mm from the centre of the space charge is 558.5kV. The continuous leader inception voltage is then calculated to be 968.8kV. The leader voltage drop is equal to 302.9kV and the 50% breakdown voltage is 1496kV.

If this 50% breakdown voltage is compared with that in section *3.3 The Breakdown Voltage* for a 7m rod-plane gap where the space charge magnitude was 5μC, the values are seen to be almost identical, the only differences being due to rounding error. It can hence be concluded that changing the magnitude of the space charge has no effect on the results of the breakdown voltage. The reason for this is due to the image charges of the space charge being scaled by the same magnitude as the space charge resulting in a zero net effect due to a change in the space charge magnitude.

D.1.3 Changing the Rod-Plane Space Charge Radius

The default radius for the space charge in all tests done using the charge simulation method is 1mm. The radius of the space charge is increased to 10mm. The gap distance between the rod tip and the plane is kept at 7m and the centre of the space charge is at 100mm from the rod tip. The results for the total induced voltage is given in *Appendix C.2.3*.

The total induced voltage 80mm from the centre of the space charge is 558.5kV. The continuous leader inception voltage is thus calculated to be 968.7kV. The leader voltage drop is 302.9kV and the 50% breakdown voltage is 1496kV.

There is little difference between the 50% breakdown voltage using a space charge with a 10mm radius as used in this test and a space charge with a mm radius as used in section *3.1.2.2 A 7m Rod-Plane Gap* and hence it can be concluded that the space charge radius has no influence on the breakdown voltage when using the charge simulation method.

D.2.1 Changing the Value of 's' in the Conductor-Plane Model

The default value for *s* which has been used in the conductor-plane model is 200mm. The effect of changing the value of *s* to 100mm in a 6m conductor-plane gap is now examined and the results for the 50% breakdown voltage are compared with that in section *4.3 The Breakdown Voltage* for a 6m conductor-plane gap which has the space charge positioned at 200mm from the base of the conductor. The results for the total induced voltage are listed in *Appendix C.3.1*.

The total induced voltage 80mm from the centre of the space charge is 474.6kV. Thus, the continuous leader inception voltage is 1321kV. The leader voltage drop is 203.7kV and the 50% breakdown voltage is 1675kV.

Comparing this value for the 50% breakdown voltage with that obtained is section *4.3 The Breakdown Voltage*, it can be seen that there is no difference in the voltage magnitudes. Hence, changing the position of the space charge in the conductor-plane model has no effect on the 50% breakdown voltage.

D.2.2 Changing the Conductor Radius

The default conductor radius is 16mm. A test was carried out where the conductor radius was changed to 6mm to study the effect which the conductor radius had on the breakdown voltage. A 6m conductor-plane gap was used with the space charge positioned at 200mm from the base of the conductor. The result of the 50% breakdown voltage is compared with that in section *4.3 The Breakdown Voltage* where the conductor radius is 16mm. *Appendix C.3.2* lists the results for the total induced voltage.

The total induced voltage 80mm from the centre of the space charge is 515.5kV. Thus, the continuous leader inception voltage is 1300kV. The leader voltage drop is 210.0kV and the 50% breakdown voltage is 1659kV.

This value for the 50% breakdown voltage is lower than that in section *4.3 The Breakdown Voltage* which is expected since a smaller conductor will result in a slightly larger E-field gradient around the conductor and hence cause leader inception and consequently breakdown to occur at a lower value.

D.2.3 Modelling a Conductor-Bundle to Plane Gap

Instead of using a single conductor in the conductor-plane gap, an investigation was made to see whether Rizk's model could be applied to calculate the breakdown voltage for the conductor-bundle to plane configuration. The single conductor is therefore replaced by four conductors in a square setup, each of the same radius, 16mm, as the single conductor and with a separation of 128mm between each other. Hence, the effective equivalent radius of a single conductor representing the setup of the four conductors would be approximately 72.2mm. The space charge was placed at a distance of 800mm from the base of the lower conductors and the gap length between the base of the lower conductors and the plane was 6m. The results for the total induced voltage is given in *Appendix C.3.3.*

The total induced voltage measured at a distance of 80mm from the centre of the space charge is 543.7kV. The continuous leader inception voltage, using the equivalent conductor radius of 72.2mm, is 1372kV. The leader voltage drop is 187.6kV and the 50% breakdown voltage is 1713kV.

Comparing this value for the 50% breakdown voltage with that measured in practice for the same geometry [Paris] which is 1770kV, the simulation result is conservative with a 3.2% error. Thus it is concluded that Rizk's model for a conductor-plane gap can be used to model a conductor-bundle to plane gap.

D.3.1 The Tower Window Structure with Three Planes

A tower-conductor gap where the tower window structure has three planes - two side planes and a top plane - is tested in order to verify the Rizk model for an additional tower-conductor gap other than that described in *Chapter 5* where the tower window structure has four planes surrounding the conductor.

The geometry of the tower-conductor gap and the materials used is exactly the same as that for the 5m tower-conductor gap studied in *Chapter 5* with the exception of the window structure only having three planes which are at ground potential and hence also only three images of the conductor, the insulator strings and the space charge. The results for the total induced voltage are listed in *Appendix C.4.1*.

The total induced voltage measured at a distance of 80mm from the space charge between the space charge and the conductor is 104.2kV. The continuous leader inception voltage is then 1205kV. The leader voltage drop is 168.4kV and the 50% breakdown voltage is 1509kV.

The result for the 50% breakdown voltage is compared with data measured in practice [Gallet, Leroy, Lacey & Kromer] where the minimum value for the U_{50} is given as 1530kV. The percentage error between the theoretical and practical values is 1.38%. Thus, the model of Rizk is again verified for the tower-conductor gap where the 50% breakdown voltage is conservative with respect to practical data.

D.3.2 The Tower-Conductor-Bundle Configuration

With the Rizk model being verified for conductor-bundle to plane gaps as well as for tower-conductor gaps, an investigation was made as to whether the model of Rizk could be applied to determine the breakdown voltage for tower-conductor-bundle gaps.

The tower window structure was modelled with three planes - two side planes and a top plane - all at ground potential, and hence producing three groups of images for the

conductor, the insulator string and the space charge. The same V-string glass insulators were used as in *Chapter 5* with each insulator string being 6m in length. The conductor bundle consisted of four 80m long conductors, spaced 457.2mm apart from each other. Each conductor had a radius of 57.15mm. If the bundle of conductors were replaced by a single conductor, the effective equivalent radius of the single conductor would be 257.9mm. The shortest distance from the side of a conductor to a ground plane was 5m. A magnitude of 5μC was given to the space charge which was placed at a distance of 1350mm from the centre of the conductor-bundle. The results for the total induced voltage are given in *Appendix C.4.2*.

The total induced voltage measured at a distance of 81mm from the centre of the space charge was 529.4kV. Using the equivalent radius of a single conductor, the continuous leader inception voltage is 1331kV. The leader voltage drop is 125.6kV and the 50% breakdown voltage is 1601kV.

Data obtained for the 50% breakdown voltage [Dillard & Hileman] shows that for the same configuration breakdown occurs at 1590kV. The value for the breakdown voltage obtained from the Rizk model is slightly higher than that obtained practically with the difference being a mere 0.656%. Thus, the Rizk model is suitable for determining the breakdown voltage for tower-conductor-bundle gaps although a small safety factor should be considered so that the models results are conservative with respect to practical data.

Author: Ehlers, Richard.
Name of thesis: Determining the switching impulse breakdown voltage over large air gaps with an application to tower-conductor window configurations.

PUBLISHER:
University of the Witwatersrand, Johannesburg
©2015

LEGALNOTICES:

Copyright Notice: All materials on the University of the Witwatersrand, Johannesburg Library website are protected by South African copyright law and may not be distributed, transmitted, displayed or otherwise published in any format, without the prior written permission of the copyright owner.

Disclaimer and Terms of Use: Provided that you maintain all copyright and other notices contained therein, you may download material (one machine readable copy and one print copy per page)for your personal and/or educational non-commercial use only.

The University of the Witwatersrand, Johannesburg, is not responsible for any errors or omissions and excludes any and all liability for any errors in or omissions from the information on the Library website.